Chapter 8

One-Dimensional Structural Properties of Proteins in the Coarse-Grained CABS Model

Sebastian Kmiecik and Andrzej Kolinski

Abstract

Despite the significant increase in computational power, molecular modeling of protein structure using classical all-atom approaches remains inefficient, at least for most of the protein targets in the focus of biomedical research. Perhaps the most successful strategy to overcome the inefficiency problem is multiscale modeling to merge all-atom and coarse-grained models. This chapter describes a well-established CABS coarse-grained protein model. The CABS (C-Alpha, C-Beta, and Side chains) model assumes a 2–4 united-atom representation of amino acids, knowledge-based force field (derived from the statistical regularities seen in known protein sequences and structures) and efficient Monte Carlo sampling schemes (MC dynamics, MC replica-exchange, and combinations). A particular emphasis is given to the unique design of the CABS force-field, which is largely defined using one-dimensional structural properties of proteins, including protein secondary structure. This chapter also presents CABS-based modeling methods, including multiscale tools for de novo structure prediction, modeling of protein dynamics and prediction of protein–peptide complexes. CABS-based tools are freely available at http://biocomp.chem.uw.edu.pl/tools

Key words Protein modeling, Protein simulations, Force-field, Statistical potentials, Knowledge-based potentials

1 Introduction

In the last two or three decades, we have been witnessing incredible progress in experimental and theoretical molecular biology. Thanks to intensive experimental studies, especially genome projects, huge amounts of sequence data (primary structures of proteins, nucleic acids, and other biomacromolecules) are now available. The combination of new experimental techniques and theoretical tools for their interpretation also provides structural (three dimensional) data for many biological macromolecules. Nevertheless, experimentally determined structures remain unknown for an increasing fraction of known protein sequences (but also other biomacromolecules). The explanation of this growing gap is simple: sequencing is now easier, faster, and less expensive than structure determination.

Yaoqi Zhou et al. (eds.), *Prediction of Protein Secondary Structure*, Methods in Molecular Biology, vol. 1484,
DOI 10.1007/978-1-4939-6406-2_8, © Springer Science+Business Media New York 2017

Deeper understanding of the molecular basis of life processes requires not only determination of structures of single biomacromolecules but also realistic pictures of their interaction with other biomacromolecules, mechanisms of assembly processes, and structural and dynamic properties of resulting complexes. Taking into consideration that we know experimental structures of only a fraction of monomeric proteins, and that the estimated number of possible protein dimers (oligomers) is an order of magnitude larger than the number of monomers, it becomes obvious that structural biology needs strong support from theoretical studies. Efficient methods for structure prediction, and modeling of dynamics and interaction are necessary. Many important problems of molecular biology can be studied using classical all-atom molecular dynamics (MD) methods. For very small and fast folding proteins it is now possible to simulate the entire folding process using superfast dedicated computers [1]. For larger systems it is still beyond capability of the available computing technology, and the time gap is huge. This is the main reason for the development of new molecular modeling tools that can handle large systems. Simplified coarse-grained, and thereby computationally very fast, models can be used for simulations of large biomacromolecules and/or for the modeling of long time processes [2, 3]. Useful coarse-grained models need to be of sufficient resolution, enabling reasonable connection with atomistic pictures [3, 4]. The high importance of such methods has been recognized a long time ago [5], resulting in the plethora of new molecular modeling tools. Recently, "*the development of multiscale models for complex chemical systems*," a pioneering work of Karplus, Levitt, and Warshel, was awarded the Nobel Prize in Chemistry for 2013.

Several very efficient coarse-grained protein models have been developed. Some of them, such as Rosetta [6, 7] or I-Tasser [8, 9], are targeted onto structure prediction, while others, such as CABS [10, 11] or UNRES [12, 13], are more universal, enabling not only structure modeling but also realistic simulations of the dynamic properties of protein systems.

The methods presented in this chapter are based on the CABS (C-Alpha, C-Beta, and Side chains) discrete representation of protein chains. Two quite fundamental features make CABS qualitatively different from other coarse grained models. The first one is that the coordinates of the model chains are restricted to discreet positions in a simple three dimensional lattice. Lattice spacing is small enough to ensure good resolution of chain representation, and large enough to make possible predefinition (and storage as integer numbers in large data tables) of all possible local conformations. This way, due to the simple computation of local moves and related energy changes, the Monte Carlo dynamics simulations are much faster than it would be possible for otherwise equivalent continuous models. The second unique feature of CABS is its interaction scheme. The force field consists of knowledge-based statistical potentials derived from the regularities observed in the known protein structures. All interactions, especially those between side chains, are treated as context-dependent. This way complicated multi-body effects are encoded in pairwise potentials. The potentials describing the energies of side chain–side chain interactions depend on the secondary structure of the interacting fragments, their mutual orientations and on the distance (short distance contacts only are treated in the explicit fashion) between side chain centers. Such a context-dependent model of pairwise interactions, especially its dependence on secondary structure, encodes the averaged effects of many physical interactions, and all these interactions, including complex interactions with the solvent, are treated in an implicit fashion.

The coarse-graining level of the CABS model enables fast and realistic reconstruction of atom level structure representation, enabling efficient multiscale modeling of protein systems [4]. The CABS model has proven to be a good tool for the computational prediction of three-dimensional protein structures, including de novo and comparative modeling, studies of protein dynamics and folding pathways, and flexible docking.

This chapter is organized as follows. In the Subheading 2 we describe the CABS protein structure representation, its force field and the sampling method. Special attention is given to the context-dependent force field of the model, which is strongly dependent on the one-dimensional properties of protein chains, especially their secondary structure assignments.

In the Subheading 3, we list and briefly describe various protein modeling methods based on the CABS model with the emphasis on those utilizing sequence and secondary structure data only. These methods include publicly available modeling tools: CABS-fold: server for protein structure, including de novo modeling and comparative modeling using one or more structural analogs [14]; CABS-dock: server for the flexible docking of peptides to proteins using no knowledge about the binding site [15, 16]; and pyCABS: software package for the simulation and analysis of long-term protein dynamics of globular proteins [17]. In the Subheading 4, we present example performance of CABS-fold, CABS-dock and pyCABS, together with short descriptions of their input requirements and options.

Finally, the Subheading 5 provides several specific comments about the modeling results obtained using CABS-based methods, their further utilization, interpretation, or alternative modeling techniques that may enhance modeling accuracy.

2 Materials

2.1 CABS Model: Coarse Grained Representation of Protein Structure

The CABS model is a universal tool for the modeling of protein structure dynamics and protein molecular docking. The main chain of protein structure is represented by a chain of Cα-atoms and pseudo atoms representing the center of virtual Cα–Cα bonds (*see* Fig. 1a, b). The latter one is needed for the simplified definition of hydrogen bonds. Side chains are represented by Cβ atoms and pseudo-atoms representing the centers of the remaining portions (where applicable) of the amino acid side chains. The CABS Cα trace is placed onto a lattice network with 0.61 Å spacing. This lattice representation significantly speeds up the Monte Carlo sampling scheme when compared with continuous models of similar resolution. The lattice spacing of 0.61 Å enables a large set of allowed orientations of Cα–Cα virtual bonds (when a slight fluctuation of their length is allowed) and thereby eliminates any noticeable orientation biases that are present in simple lattice models. The average accuracy of the Cα-trace representation is about 0.35 Å, and slightly depends on the secondary structure patterns of the proteins studied (*see* Fig. 1c).

2.2 Force Field of the CABS Model with Secondary Structure Context-Dependent Statistical Potentials

The force field of CABS is constructed from knowledge-based statistical potentials, derived from the structural regularities (and their relation to the amino acid sequences) seen in protein structures collected in databases. A large representative set has been used for the derivation of all potentials. The weight of various potentials is properly tuned by optimizing the total energy of folded structure and other properties of the model, for instance secondary structure content at folded and unfolded structures of the proteins being modeled. The details of the force field of CABS models and the motivations for specific choices of their potentials have been described previously [10]. Here we outline the general ideas behind this force field, focusing on the crucial role of secondary structure assignments for the model and its force field.

Protein chain geometry in the CABS model is fully encoded by its Cα-trace, where positions of all Cα atoms are restricted to the points of the underlying cubic lattice grid. The planar angles between two subsequent Cα–Cα pseudo-bonds are restricted to values seen in protein structures. Sequence-independent and sequence-dependent potentials enforce distribution of this angle typical for the distribution seen in globular proteins. The angles of rotation of three consecutive Cα–Cα pseudo-bonds are similarly treated. This way, for instance, left-handed helix-like conformations are treated as unlike. The sequence dependence of the angular potentials is not straightforward, and it does not come from a specific identity of three or four residue fragments, but from the predicted secondary structure which depends on much

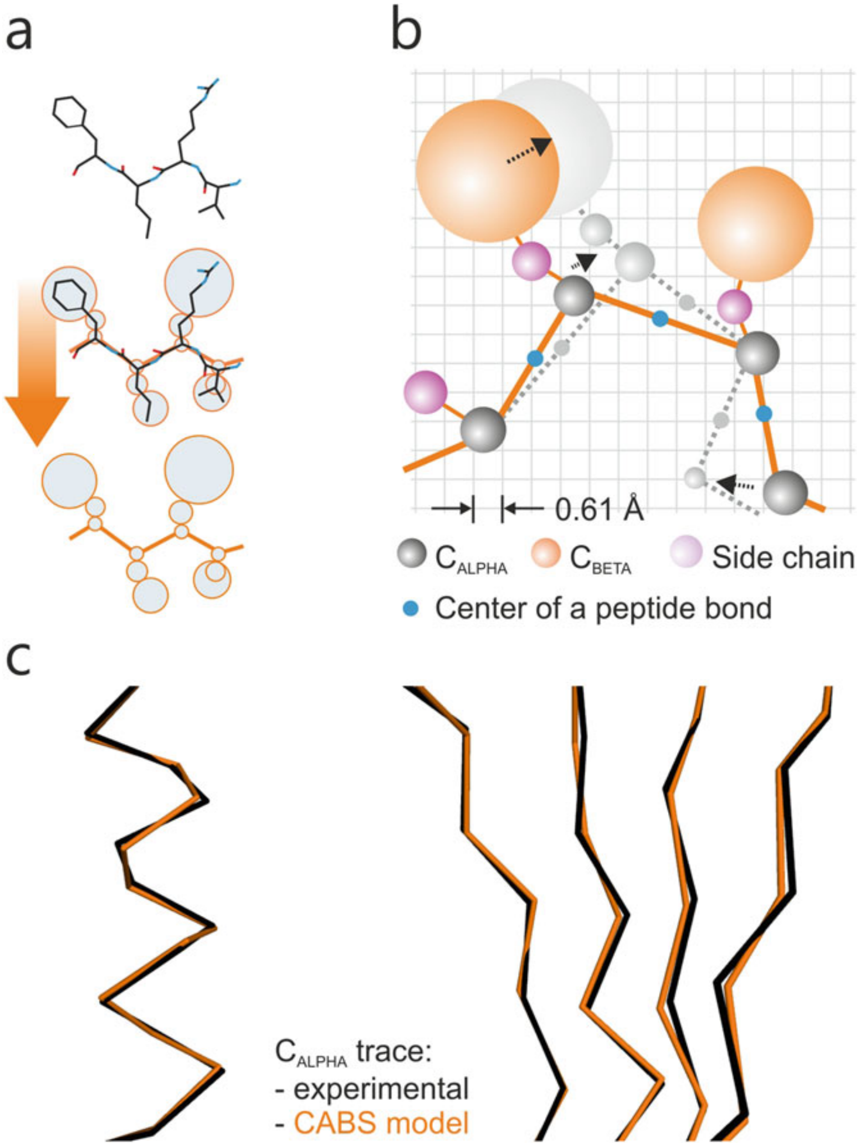

Fig. 1 Representation of a protein chain in the CABS model. (**a**) scheme showing conversion from all-atom to coarse-grained CABS representation, (**b**) details of CABS coarse-grained representation, (**c**) comparison of the C-alpha trace in experimental protein structure (*black* color) and after conversion to CABS representation (*orange*) presented here for an example helix and beta sheet secondary structure (experimentally derived C-alpha coordinates of both secondary structure motifs were taken from the 2GB1 PDB file)

longer protein fragments. This way complex multibody interactions are encoded in this simple potential. Positions of Cβ carbons (not restricted to the lattice) are defined by the positions of three consecutive Cα atoms for the Cβ bound to the central Cα. These positions depend on the planar angles between the Cα–Cα pseudobonds. Cα and Cα united atoms are treated as rigid bodies. Virtual united atoms, placed at the center of atom-Cα pseudo-bonds, define the positions of the main chain hydrogen bonds in the form of attractive, orientation-dependent contact potentials of the same strength for all residues belonging to the same predefined secondary structure assignment. Other hydrogen bonds have the same geometry, but are considered weaker, with a smaller weight factor. The excluded volume spheres of united Cα, Cβ atoms and hydrogen bonds forming pseudo-atoms are slightly smaller in the CABS model than the distance of a corresponding strong repulsive interaction in real proteins. This is necessary to enable non-perfect dense packing in the native-like structure of the modeled proteins. Positions of centers of the remaining portion of amino acid side chains (where applicable) are also taken from tables defined for specific amino acids and local angles of the Cα-trace. Interactions between the centers of amino acid side chains are most important for the performance of the CABS model. Side chains are treated as soft excluded volume bodies at short distances, and interacting through contact potential at a longer distance. The width of contact distance is about 2 Å. The soft excluded volume of the side chains and the width of the contact range cover the potential problems with non-accurate representation of side chain conformations, especially for larger amino acids.

Side chain pairwise contact potentials are crucial for the performance of the CABS model. These statistical potentials are context dependent, and the strength of pairwise interactions depends on the mutual orientation of the interacting side chains and on the geometry of the nearest fragments of the main chain backbone. Here we discuss and present this potential for single domain globular proteins. It is important to note that the reference state in the derivation of CABS statistical potentials is a compact state of protein chains with a random sequence of the same composition as the protein of a given composition. Similar context-dependent potentials can be derived for interactions between globular proteins, transmembrane proteins, etc. It means that the CABS force field is not easily "transferable," it is rather "expandable" for an increasing range of modeled systems. We do not consider this a strong disadvantage of "knowledge-based" statistical potentials. "Transferability" of "physics-based" force fields for reduced models is also not trivial [18].

The idea of the context-dependent classification of side chain contacts is illustrated in Fig. 2 and numerical data are presented in Tables 2–10. The mutual orientation of the contacting side chains is divided into three ranges: near-antiparallel, intermediate, and near parallel (Fig. 2a). The local geometry of the main chain of a contacting residue is classified in the CABS force field into two classes: compact and expanded. This way the secondary structure prediction (or assignment) defines the specific energy of side chain interactions. For example: an antiparallel contact of two residues with a compact geometry of the corresponding elements of the main chain backbone usually means a helix-helix contact, while a parallel contact of side chains from two expanded elements of the

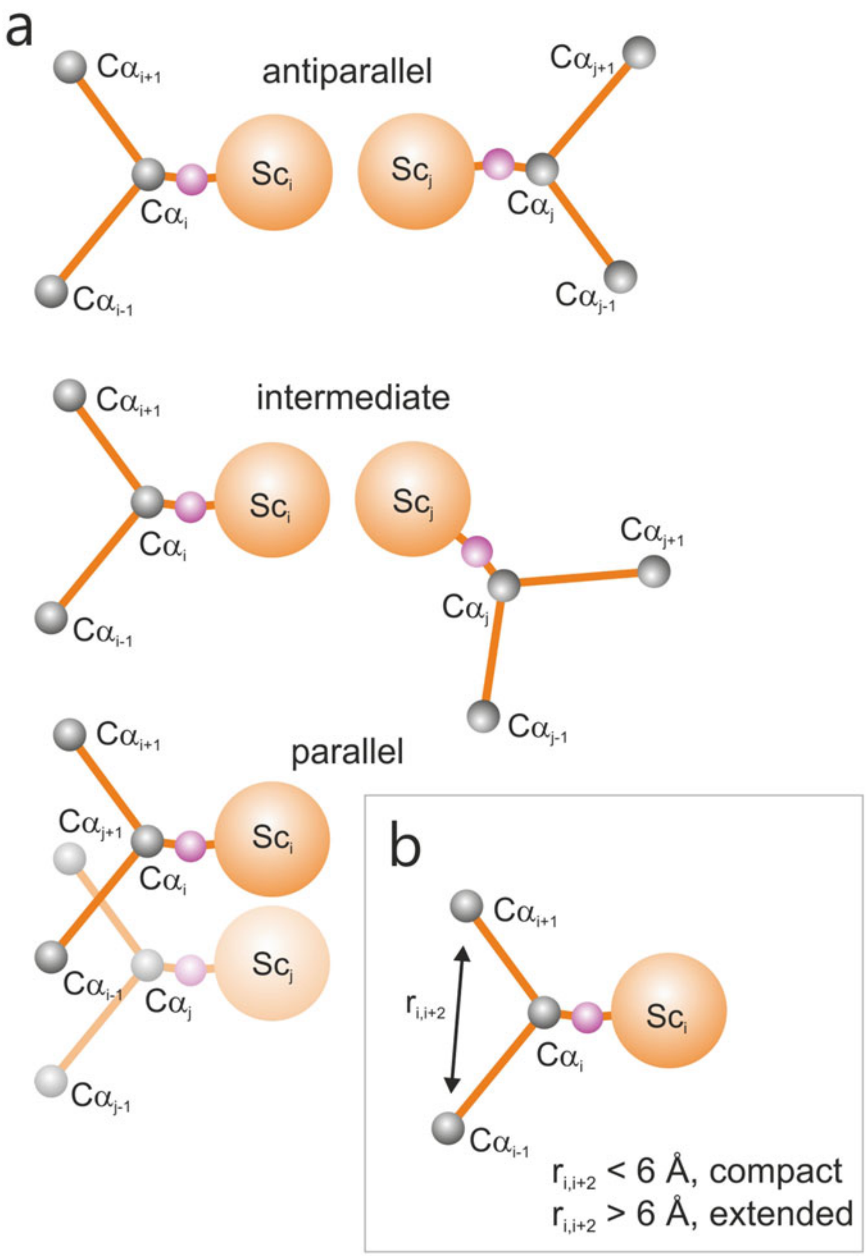

Fig. 2 Types of protein structure arrangements used in the definition of sequence-dependent pairwise potentials. (**a**) Three types of mutual orientations of the side chains (antiparallel, medium-intermediate, parallel). (**b**) Two types of main chain conformations (helical-compact and expanded-beta). Numerical values of the potentials are given in Tables 2–10

main chain usually comes from two adjoined beta strands. The context-dependent contact potentials of the CABS force field differ qualitatively from the other potentials (probably all of them) used in protein modeling. In the majority of these potentials the contact energy for two oppositely charged amino acids will suggest weak attractive interactions of their side chains. In the CABS force field (for single-domain globular proteins) interactions of such pairs of residues are treated as strongly attractive for a parallel contact and strongly repulsive for an antiparallel contact of the side chains. Since the solvent in the CABS model force field is treated in a strictly implicit fashion (which is also the case for the majority of other statistical potentials) such orientation-dependent strength of interactions is not surprising. Charged residues are usually located on the surface of a protein globule, where they cannot form antiparallel contacts. If they are located (which is rather rare) more in the center of a globule, it is most likely that it is a binding site, where charged residues are on the surface of the binding site. Also in this case the parallel contact is more probable.

As discussed above, the predicted (or assigned) secondary structure in a three-state version (helix, beta, other) is crucial for CABS force field statistical potentials. This unique feature of the CABS coarse-grained modeling approach is a strength of the model, with very few drawbacks. The model has proved to be very efficient in de novo protein structure assembly simulations, comparative modeling support, modeling of protein dynamics and interactions with other biomolecules. In the last case the force field needs to be properly expanded, including for example contact potentials between side chains from two protein (peptide) chains. Due to the qualitative difference between CABS side chain contact potentials and other statistical potentials, we decided to attach its numerical data presented in nine tables (numbered from Tables 2–10). Two-digit accuracy is sufficient for most applications of this potential.

The contact potentials data (Tables 2–10) are potentially very useful not only in coarse-grained modeling (with model resolution similar to that assumed in the CABS model) but also as a source for definition/sorting of many other one-dimensional, two-dimensional, and three-dimensional protein features. For instance it is possible to use the numerical data of this potential for the classification of burial patterns of protein sequences. The potential can also be used in efficient threading algorithms, and in other structural bioinformatics methods. Additional comments on the meaning of the tables and accessibility in software packages are provided in **Note 1**.

2.3 Sampling Schemes

The Monte Carlo sampling scheme of CABS is a series of local, randomly selected, small conformational transitions onto the underlying lattice. The set of local changes of model chain coordinates includes single Cα moves (*see* Fig. 1b), moves of two Cα fragments, and rarely attempted small distance moves of longer fragments of the model chains. Chain ends are treated separately. Due to lattice discretization of the Cα coordinates (800 of allowed orientations of Cα–Cα pseudo-bond vectors) the possible local moves could be stored in large data tables and thereby local moves do not require any costly computations of trigonometric functions. Local moves require just simple random sorting of predefined sequences of integer numbers. This way the discrete (restricted to a high coordination lattice) representation of chain conformations makes the CABS model computationally much faster in comparison to otherwise equivalent continuous coarse-grained models. The geometry of the main chain defines the positions of the side chain united atoms (not restricted to the lattice). A library of these positions is predefined by sorting and averaging PDB structures for all possible amino acid sequences of the central and two neighboring elements of the Cα–trace. All random moves are accepted according to the Metropolis criteria. Since the randomly selected moves mimic fast local conformational fluctuations of the modeled protein chains, their long series provides a realistic picture of the long time dynamics of modeled systems. CABS-based modeling schemes can use simple MC dynamics simulations at a given temperature, MC simulated annealing, and various versions of Replica Exchange (REMC) simulations. The CABS model (MC dynamics or REMC) could be easily combined with all-atom molecular dynamics. Several simple algorithms, classical and specifically targeted onto CABS representation, can be used for the fast and realistic reconstruction of atomistic representation, suitable for classical MD simulations (*see* **Note 2**). This way CABS can be used as a very efficient engine in multiscale protein modeling schemes. The basic structure of multiscale modeling procedures with CABS is illustrated in Fig. 3. Some helpful tools for the analysis of derived models and CABS trajectories are presented in **Notes 3** and **4**.

3 Methods

In the last several years, CABS coarse-grained protein models have become a key component in various multiscale modeling methods. Those methods generally follow a similar pipeline merging CABS simulations (usually the first modeling step) and all-atom modeling (final modeling steps), as presented in Fig. 3.

The CABS-based modeling methods have three application areas:

1. Protein structure prediction: homology modeling [14, 19–21], ab initio prediction of small proteins [14], or protein loops/fragments [22–24] (in ref. [23] also in combination with the classical Modeller tool [25]), modeling based on sparse experimental data [26].
2. Prediction of protein complexes: protein–peptide [15, 16, 27] and protein–protein [28, 29].
3. Efficient simulation of protein dynamics: protein folding mechanisms [4, 11, 30–34] and flexibility of globular proteins [35–38].

In all these applications, the CABS model serves as a highly efficient simulation engine that allows CABS-based methods to be much cheaper in terms of CPU time (in comparison to classical

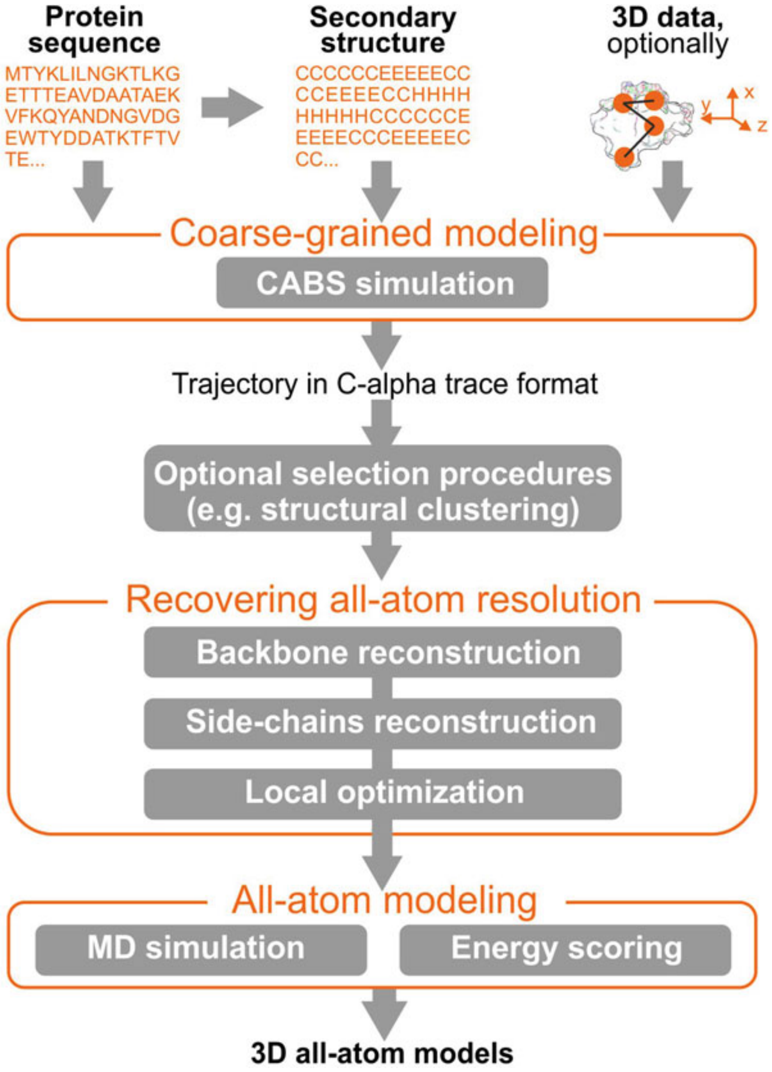

Fig. 3 Typical stages of the multiscale modeling scheme utilizing the CABS model. The modeling input includes one dimensional data (protein sequence and secondary structure) and, optionally, three-dimensional data (e.g., distance restraints from experiment or from evolutionary analysis). Secondary structure data are required in a three-letter code (C, coil; E, extended; H, helix). The modeling scheme consists of three major stages: (1) coarse-grained modeling with the CABS model, (2) several steps of reconstruction to all-atom representation, and (3) all-atom modeling procedures (e.g., simulation using all-atom MD or all-atom energy scoring)

modeling tools [35]), or to achieve sampling efficiency that exceeds other existing approaches. For example, the CABS-dock method for the molecular docking of peptides to proteins enables docking fully flexible peptides to flexible receptors without prior knowledge of the binding site [15, 16]. In practice, CABS-dock performs simulation of coupled folding and binding during which peptides have a possibility to explore the entire surface of a protein receptor. Presently, there are no other simulation methods enabling exploration of such a large conformational space in a reasonable time. In contrast to CABS-dock, other state-of-the-art protein–peptide docking methods are restricted to a specified binding site, or to very short peptides (2–4 amino acids, while CABS-dock has been successfully tested on a large set of peptides with 5–15 amino acids [15, 16]).

Table 1
Performance of the CABS-based modeling methods in ab initio prediction tasks (utilizing one dimensional data only: protein sequence and secondary structure)

Method and availability	Benchmark set	Performance summary
Prediction of protein structure or protein fragments		
CABS-fold server for the ab initio and consensus-based prediction of protein structure [14]. Available as a web server at: http://biocomp.chem.uw.edu.pl/CABSfold/	Methodology validated during CASP competitions as one of the leading approaches [19–21], applied to the ab initio modeling of large protein fragments or entire proteins (with or without 3D restraints)	Small proteins (up to 100 residues long) or peptides can be predicted with high accuracy (up to 2 Å) or medium accuracy (up to 5 Å) The CABS-fold server can also be used to predict protein loops (see the performance below)
Method(s) for predicting protein loops in globular proteins [23]	From 186 experimental protein structures, covering all the structural classes of proteins, internal loops of various length (from 4 to 25 residues) have been removed and treated as unknown	Performance was compared with two classical modeling tools: Modeller [25] and Rosetta [6]. Modeller performance was usually better for short loops, while CABS and Rosetta were more effective for longer loops (resolution of such models was usually on the level of 2–6 Å)
Prediction method for protein loops in GPCR membrane receptors [24]	From 13 experimental GPCR receptor structures, extracellular second loops (between 13 and 34 residues) have been removed and treated as unknown. The benchmark set is available at: http://biocomp.chem.uw.edu.pl/GPCR-loop-modeling/	Resolution of the best models obtained (among many others) was on the level of 2–6 Å, while the best scored models were on the level of 2–8 Å. Performance was comparable to that of other state-of-the-art methods [24]

(continued)

Table 1 (continued)

Method and availability	Benchmark set	Performance summary
Method for protein fragment reconstruction [22]	From 20 protein structures of various structural classes, protein fragments (from 10 to 29 residues) have been removed and treated as unknown	Resolution of the resulting models was on the level of 1.5 and 6 Å. Performance was compared with SICHO [53], Refiner [22], Swiss-model [54] and Modeller [25] methods. CABS, SICHO and Refiner performance was usually better than for Swiss-model and Modeller
Protein–peptide molecular docking and binding site prediction (using no knowledge about the peptide structure)		
CABS-dock method for molecular docking with no knowledge of the binding site [15, 16]. Available as a web server at: http://biocomp.chem.uw.edu.pl/CABSdock/	Benchmark set of nonredundant (<70 % sequence identity with respect to the receptor protein) protein–peptide interactions (108 bound and 68 unbound receptors) with peptides of 5–15 amino acids [55]. The benchmark set is available at: http://biocomp.chem.uw.edu.pl/CABSdock/benchmark	For over 80 % of bound and unbound cases high or medium accuracy models were obtained (high accuracy: peptide-RMSD<3 Å; medium accuracy: 3 Å ≤ peptide-RMSD ≤ 5.5 Å; where peptide-RMSD is the RMSD to the experimental peptide structure after superimposition of receptor molecules
Ab initio protocol for studying the folding and binding mechanism of intrinsically disordered peptides [27]	pKID-KIX protein complex (pKID is a 28 residue disordered peptide which folds upon binding to the KIX domain)	An ensemble of transient encounter complexes obtained in the simulations was in good agreement with experimental results
Prediction of protein folding mechanisms		
pyCABS protocols for efficient simulations of long-time protein dynamics [17]. Software package available at: http://biocomp.chem.uw.edu.pl/pycabs/	Tested in protein folding studies of small (up to 100 residues long) globular proteins [4, 11, 30–33]	The views of denatured ensembles of protein structures obtained in the simulations were in good agreement with the experimental measurements of protein folding [4, 11, 30–33]
Multiscale protocol merging efficient simulations with CABS and replica exchange all-atom MD [34]	β-Hairpin from the B1 domain of protein G (PDB code: 2GB1, residues 41–56)	Combination of CABS and all-atom MD simulations significantly accelerates system convergence (several times in comparison with all-atom MD starting from the extended chain conformation)

In Table 1, we list the CABS-based methods that enable protein structure modeling based on one-dimensional data only (sequence and secondary structure), together with their accessibility, references, benchmark information, and performance summary. For selected methods (CABS-fold [14], CABS-dock [15, 16], and pyCABS [17]), example case studies are presented in the next section.

Apart from the methods listed in Table 1, the CABS model has also been used in web server tools: CABS-flex server for the prediction of protein structure fluctuations [36, 37] and Aggrescan3D server for the prediction of protein aggregation properties and rational design [38] (Aggrescan3D uses the CABS-flex method for modeling the influence of conformational flexibility on aggregation properties). The major advantage of the CABS-flex method is its efficiency. It allows us to achieve similar results as with classical all-atom MD, but several thousand times faster [35].

4 Case Studies

4.1 Protein Structure Prediction Using the CABS-Fold Server

The CABS-fold server for protein structure prediction operates in two modeling modes: consensus modeling (based on structural templates) and de novo modeling (based only on sequence) [14]. In both modes, the secondary structure is an optional input (*see* **Note 5**): if the secondary structure is not provided, it is automatically predicted using the Psi-Pred method [39]. It is also possible to add distance restraints into the modeling process and to modify CABS simulation settings. These additional options can be accessed from the “Advanced options” input panel (*see* Fig. 4 presenting example CABS-fold screenshots).

CABS-fold performance and the benchmark summary are presented in Table 1. In Fig. 5, we present an example modeling result using the de novo modeling mode and the sequence of a small protein domain, yeast copper transporter CCC2A (72 residues). Protein sequence and secondary structure inputs are also provided in the figure. The CCC2A protein structure has been solved experimentally and has a beta–alpha–beta–beta–alpha–beta ferredoxin-like fold (PDB ID: 1fvq). Figure 5 shows a comparison of the experimental and CABS-fold predicted model with the same fold which differ in details of secondary structure packing. It is worth to mention that obtaining such a modeling result based on protein sequence only is not trivial and possible (in a reasonable computational time) only using a few coarse-grained based methods.

4.2 Protein–Peptide Docking Using the CABS-Dock Server

The CABS-dock server for modeling protein–peptide interactions [15, 16] enables efficient docking search of a peptide over

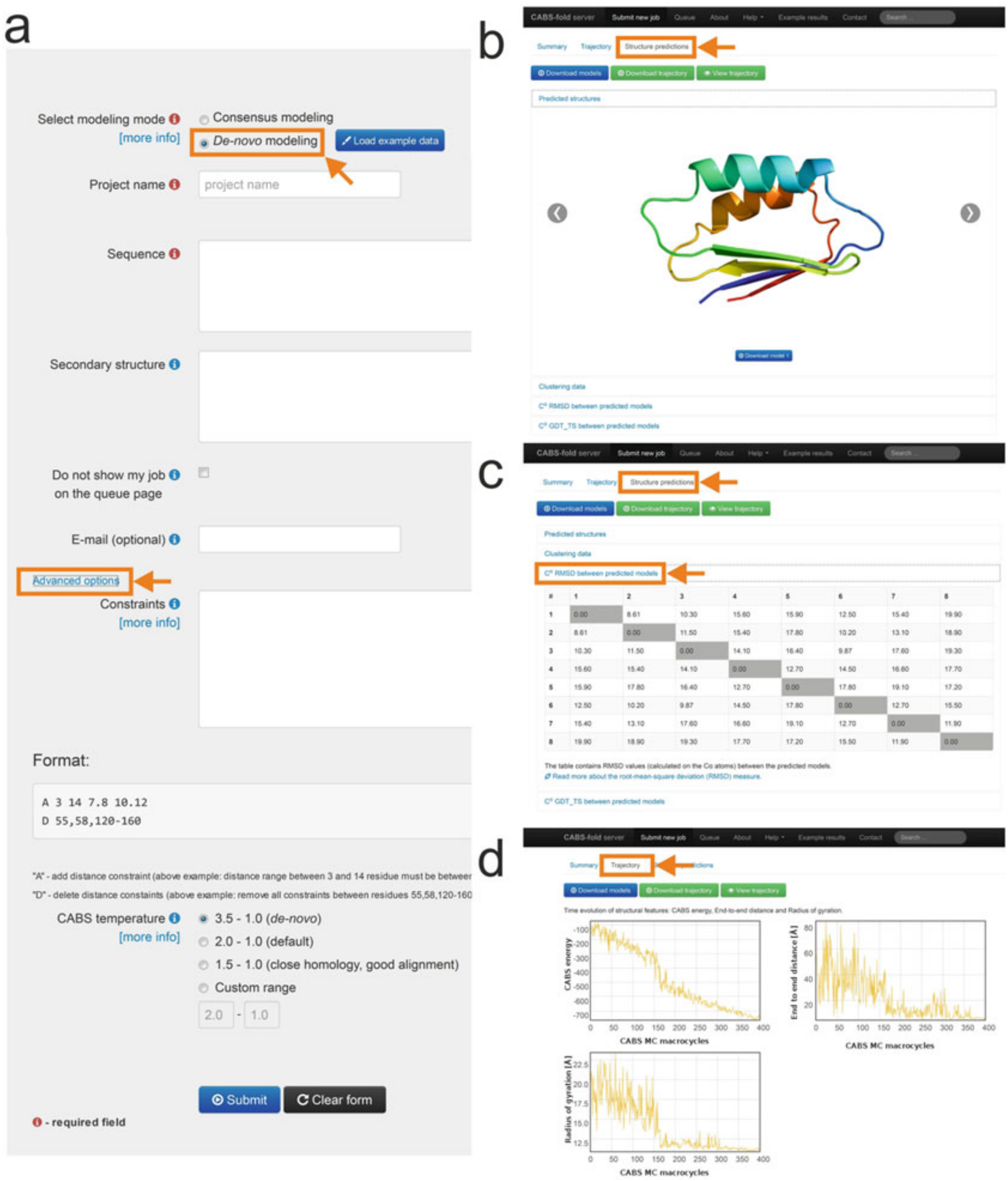

Select modeling mode: ○ Consensus modeling ● *De-novo* modeling

Project name: project name

Sequence

Secondary structure

Do not show my job on the queue page □

E-mail (optional)

Constraints

Format:

```
A 3 14 7.8 10.12
D 55,58,120-160
```

"A" - add distance constraint (above example: distance range between 3 and 14 residue must be betweer

"D" - delete distance constaints (above example: remove all constraints between residues 55,58,120-160

CABS temperature: ● 3.5 - 1.0 (*de-novo*) ○ 2.0 - 1.0 (default) ○ 1.5 - 1.0 (close homology, good alignment) ○ Custom range 2.0 - 1.0

- required field

#	1	2	3	4	5	6	7	8
1	0.00	8.61	10.30	15.60	15.90	12.50	15.40	19.90
2	8.61	0.00	11.50	15.40	17.80	10.20	13.10	18.90
3	10.30	11.50	0.00	14.10	16.40	9.87	17.60	19.30
4	15.60	15.40	14.10	0.00	12.70	14.50	16.60	17.70
5	15.90	17.80	16.40	12.70	0.00	17.80	19.10	17.20
6	12.50	10.20	9.87	14.50	17.80	0.00	12.70	15.50
7	15.40	13.10	17.60	16.60	19.10	12.70	0.00	11.90
8	19.90	18.90	19.30	17.70	17.20	15.50	11.90	0.00

The table contains RMSD values (calculated on the Cα atoms) between the predicted models.

Read more about the root-mean-square deviation (RMSD) measure.

Time evolution of structural features: CABS energy, End-to-end distance and Radius of gyration.

Fig. 4 Example screenshots from the CABS-fold server. (**a**) Main page input panel. Output panels presenting: (**b**) predicted models, (**c**) RMSD between the predicted models, (**d**) characteristics of the structure prediction trajectories. Selected/clicked options are marked with *orange rectangles* and *arrows*

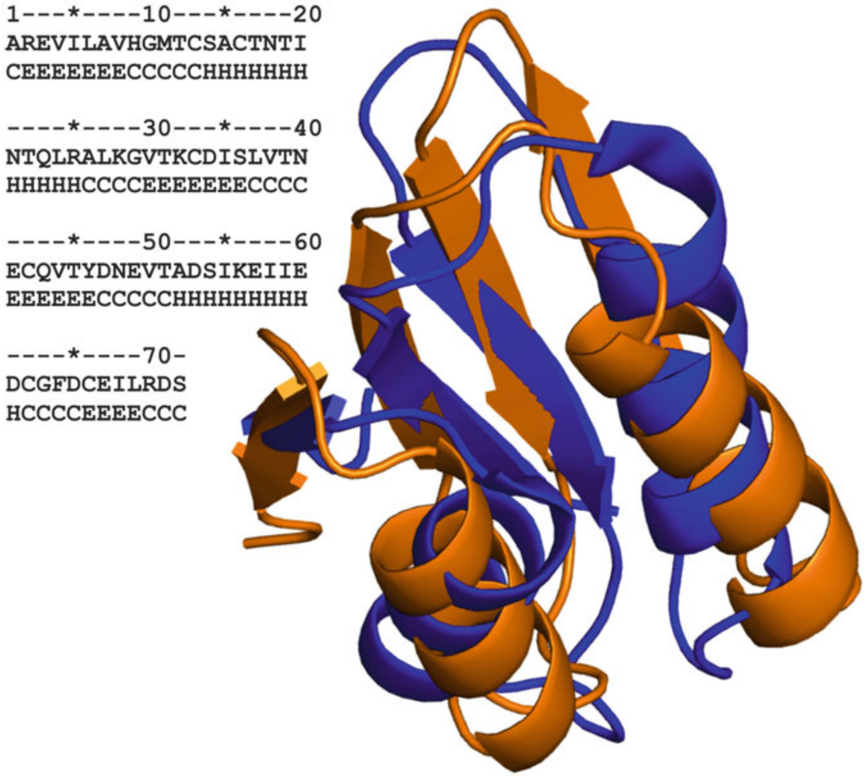

Fig. 5 Example CABS-fold structure prediction result. The only input data: protein sequence and secondary structure (predicted from sequence by the Psi-pred method [ref]) are shown on the left. The experimental structure (*blue*) of a 72 residue protein (PDB ID: 1fvq) is superimposed on the CABS-fold predicted model (*orange*). In comparison to the experimental structure, the CABS-fold model has the same fold and RMSD value is 3.7 Å

the entire protein receptor structure. During CABS-dock docking, the peptide is simulated as fully flexible, while the protein receptor structure is also flexible but only to a small extent. As an input, the CABS-dock method uses information about the peptide sequence and structure of a protein receptor. The peptide secondary structure is an optional input (*see* **Note 5**; if not provided, the method uses the PsiPred tool [39] for secondary structure prediction). Other optional inputs include the possibility to assign high flexibility for selected receptor fragments, and to exclude selected receptor fragments from docking search (these are accessible from the optional input panel, see the CABS-dock screenshots in Fig. 6).

CABS-fold performance and the benchmark summary are presented in Table 1. In Fig. 7, we present an example modeling result obtained using the optional CABS-dock feature that allows for the significant flexibility of a selected receptor fragment. In the presented modeling case, assigning significant flexibility to the flexible loop

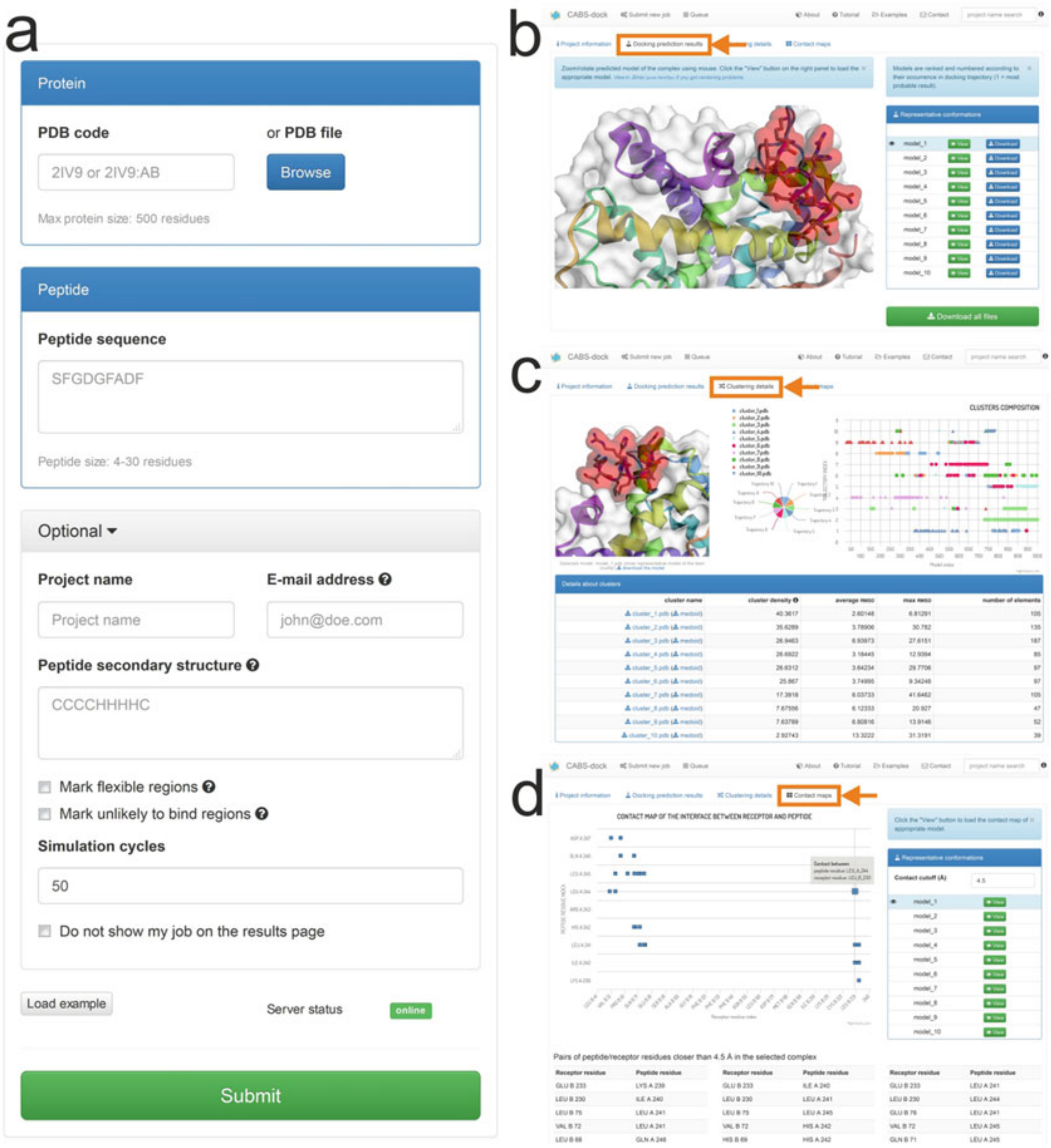

Protein

PDB code: 2IV9 or 2IV9:AB — or PDB file: Browse

Max protein size: 500 residues

Peptide

Peptide sequence: SFGDGFADF

Peptide size: 4-30 residues

Optional ▾

Project name: Project name — E-mail address: john@doe.com

Peptide secondary structure: CCCCHHHHC

☐ Mark flexible regions

☐ Mark unlikely to bind regions

Simulation cycles: 50

☐ Do not show my job on the results page

Load example — Server status: online

Submit

Zoom/rotate predicted model of the complex using mouse. Click the "View" button on the right panel to load the appropriate model.

Models are ranked and numbered according to their occurrence in docking trajectory (1 = most probable result).

Details about clusters

cluster name	cluster density	average rmsd	max rmsd	number of elements
cluster_1.pdb (medoid)	40.3617	2.60148	6.81291	105
cluster_2.pdb (medoid)	35.6289	3.78906	30.782	135
cluster_3.pdb (medoid)	26.9463	6.93973	27.6151	187
cluster_4.pdb (medoid)	26.6922	3.18445	12.9394	85
cluster_5.pdb (medoid)	26.6312	3.64234	29.7706	97
cluster_6.pdb (medoid)	25.867	3.74995	9.34248	97
cluster_7.pdb (medoid)	17.3918	6.03733	41.6462	105
cluster_8.pdb (medoid)	7.67556	6.12333	20.927	47
cluster_9.pdb (medoid)	7.63789	6.80816	13.9146	52
cluster_10.pdb (medoid)	2.92743	13.3222	31.3191	39

Click the "View" button to load the contact map of appropriate model.

Pairs of peptide/receptor residues closer than 4.5 Å in the selected complex

Receptor residue	Peptide residue	Receptor residue	Peptide residue	Receptor residue	Peptide residue
GLU B 233	LYS A 239	GLU B 233	ILE A 240	GLU B 233	LEU A 241
LEU B 230	ILE A 240	LEU B 230	LEU A 241	LEU B 230	LEU A 244
LEU B 75	LEU A 241	LEU B 75	LEU A 245	GLU B 76	LEU A 241
VAL B 72	LEU A 241	VAL B 72	HIS A 242	VAL B 72	LEU A 245
LEU B 68	GLN A 248	HIS B 69	HIS A 242	GLN B 71	LEU A 245

Fig. 6 Example screenshots from the CABS-dock server. (**a**) Main page input panel. Output panels presenting: (**b**) predicted models, (**c**) clustering results and analysis, (**d**) contact maps for predicted models. Selected/clicked options are marked with *orange rectangles* and *arrows*

(which partially blocks the binding site in the unbound input form) was crucial for obtaining a high resolution complex model.

4.3 Protein Dynamics Using the pyCABS Package

The pyCABS software package [17] is dedicated to performing long-time simulations of small globular proteins using the CABS model. The possible applications include de novo folding from a random structure (folding mechanisms), near-native dynamics, unfolding processes, and long-time dynamics of unfolded structures.

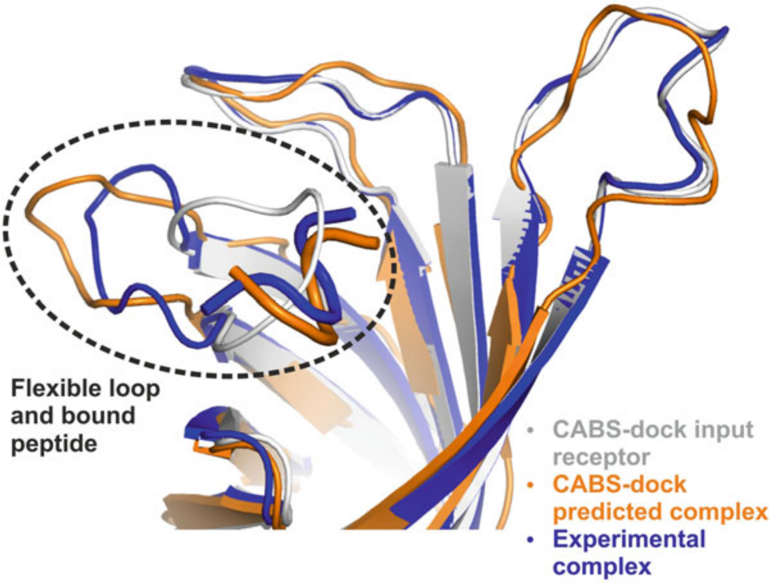
Flexible loop and bound peptide
• CABS-dock input receptor
• CABS-dock predicted complex
• Experimental complex

Fig. 7 Example result of CABS-dock protein–peptide docking using the option of significant flexibility for the selected receptor fragment. The figure shows comparison of the CABS-dock input structure in the peptide-unbound form (colored in *gray*, PDB ID: 2RTM) with a CABS-dock-predicted complex (in *orange*) and a peptide-bound experimental complex (in blue, PDB ID: 1KL3). RMSD between the predicted and experimental peptide structure is 2.03 Å. The flexible loop region (designated to be fully flexible during docking) is between residues 45 and 54

The package requires the protein sequence and its secondary structure (predicted or experimentally assigned, *see* **Note 5**) and starting structure(s): depending of the modeling goal, it can be a random structure, or a selected (e.g., native) structure.

pyCABS performance and the benchmark summary are presented in Table 1. In Fig. 8, we present an example modeling result from the simulation of folding of barnase globular protein. The simulation was performed in the de novo manner, i.e., using a random starting structure. The resulting picture of the folding mechanism matches well with the experimental data and has been described in detail in ref. [11] (the technical details for carrying out such a simulation using pyCABS are provided in ref. [17]).

5 Notes

1. Tables 2–10 are an integral part of the CABS (and pyCABS [17]) software package (stored in the “QUASI3S” text file). Each of these tables is labeled by a three-letter code (like PEE, PCC, and PCE) whose meaning is explained in Fig. 2. For

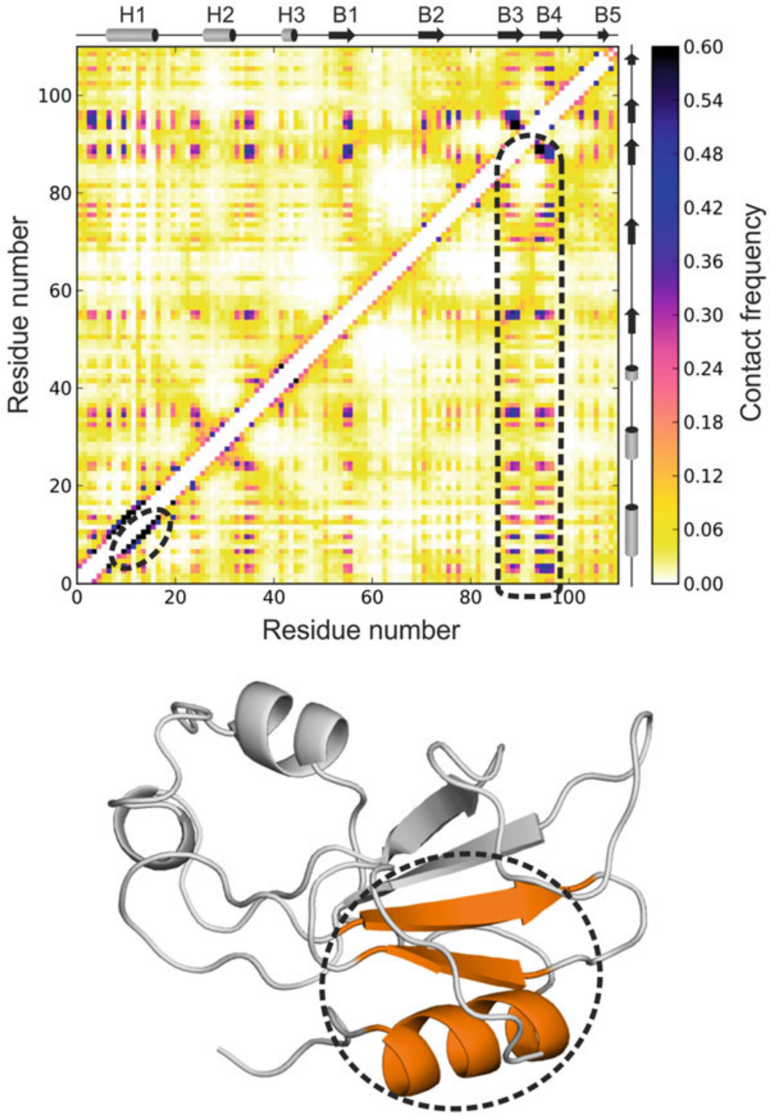

Fig. 8 Example result from simulations of long-term protein dynamics (from a fully denatured to a near-native state) using the CABS model and protein sequence only. A simulation contact map is presented showing the key step of barnase folding (PDB code: 1BNR). The presented key folding step is the formation of the nucleation site. The nucleation site is formed by the following elements of secondary structure: helix 1 and beta-strands: 3 (marked by *dashed lines* in the contact map and colored also in *orange* in the native barnase structure, shown below). The map colors indicate contact frequency (see the legend)

example, the PCE type of interactions occurs between amino acid chains forming a parallel contact (P), where the first contacting side chain (given in columns) is attached to a compact (C, most likely a helix) type of conformation and the second contacting side chain (given in rows) is attached to expanded (E, most likely beta-strand) conformation.

Table 2
Context pairwise contact potential for the PCC type of side chain interactions

PCC	GLY	ALA	SER	CYS	VAL	THR	ILE	PRO	MET	ASP	ASN	LEU	LYS	GLU	GLN	ARG	HIS	PHE	TYR	TRP
GLY	3.3	1.8	1.6	1.6	1.6	1.2	1.3	1.8	0.9	1.0	0.9	1.6	1.5	1.4	1.4	0.9	1.5	1.1	1.1	1.0
ALA	1.8	0.6	0.8	0.4	0.4	0.5	0.3	0.9	0.2	0.7	0.5	0.3	0.8	0.5	0.3	0.2	0.4	0.1	0.2	0.2
SER	1.6	0.8	0.7	0.9	0.3	0.4	0.2	0.9	0.3	0.2	0.2	0.5	0.3	0.2	0.0	−0.1	−0.1	0.1	0.0	0.0
CYS	1.6	0.4	0.9	−0.2	−0.4	0.3	−0.6	0.4	−0.6	0.9	0.4	−0.4	0.3	0.5	0.7	0.2	−0.4	−0.8	−0.6	−0.6
VAL	1.6	0.4	0.3	−0.4	−0.6	−0.3	−0.9	0.6	−0.8	0.7	−0.0	−0.9	0.1	0.2	−0.0	−0.3	−0.3	−1.0	−0.7	−1.1
THR	1.2	0.5	0.4	0.3	−0.3	−0.1	−0.5	0.7	−0.2	0.1	−0.2	−0.3	−0.1	−0.0	−0.4	−0.2	−0.2	−0.3	−0.4	−0.4
ILE	1.3	0.3	0.2	−0.6	−0.9	−0.5	−1.1	0.4	−0.9	0.5	0.1	−1.1	−0.1	−0.0	−0.2	-0.3	−0.3	−1.1	−0.7	−1.1
PRO	1.8	0.9	0.9	0.4	0.6	0.7	0.4	1.4	0.4	1.0	0.6	0.6	0.6	0.6	0.5	0.2	0.5	0.6	−0.0	−0.0
MET	0.9	0.2	0.3	−0.6	−0.8	−0.2	−0.9	0.4	−0.2	0.4	-0.1	−0.9	0.1	0.1	−0.3	−0.5	−0.7	−1.1	−0.9	−0.8
ASP	1.0	0.7	0.2	0.9	0.7	0.1	0.5	1.0	0.4	0.5	0.0	0.9	−0.6	0.5	−0.4	−0.7	−0.2	0.3	0.3	0.2
ASN	0.9	0.5	0.2	0.4	−0.0	−0.2	0.1	0.6	−0.1	0.0	0.1	0.2	−0.3	−0.1	−0.3	−0.3	−0.0	0.1	−0.1	−0.1
LEU	1.6	0.3	0.5	−0.4	−0.9	−0.3	−1.1	0.6	−0.9	0.9	0.2	−1.0	−0.0	0.2	−0.1	−0.3	−0.3	−1.1	−0.8	−0.9
LYS	1.5	0.8	0.3	0.3	0.1	−0.1	−0.1	0.6	0.1	−0.6	−0.3	−0.0	0.4	−0.9	−0.5	−0.1	0.1	−0.0	−0.4	0.0
GLU	1.4	0.5	0.2	0.5	0.2	−0.0	−0.0	0.6	0.1	0.5	−0.1	0.2	−0.9	0.2	−0.5	−1.0	−0.4	0.2	−0.1	−0.2
GLN	1.4	0.3	0.0	0.7	−0.0	−0.4	−0.2	0.5	−0.3	−0.4	−0.3	−0.1	−0.5	−0.5	−0.2	−0.5	−0.3	−0.1	−0.4	−0.7
ARG	0.9	0.2	−0.1	0.2	−0.3	−0.2	−0.3	0.2	−0.5	−0.7	−0.3	−0.3	−0.1	−1.0	−0.5	−0.2	−0.3	−0.3	−0.6	−0.5
HIS	1.5	0.4	−0.1	−0.4	−0.3	−0.2	−0.3	0.5	−0.7	−0.2	−0.0	−0.3	0.1	−0.4	−0.3	−0.3	−0.4	−0.5	−0.7	−0.8
PHE	1.1	0.1	0.1	−0.8	−1.0	−0.3	−1.1	0.6	−1.1	0.3	0.1	−1.1	−0.0	0.2	−0.1	−0.3	−0.5	−1.0	−1.0	−1.2
TYR	1.1	0.2	0.0	−0.6	−0.7	−0.4	−0.7	−0.0	−0.9	0.3	−0.1	−0.8	−0.4	−0.1	−0.4	−0.6	−0.7	−1.0	−0.5	−1.1
TRP	1.0	0.2	0.0	−0.6	−1.1	−0.4	−1.1	−0.0	−0.8	0.2	−0.1	−0.9	0.0	−0.2	−0.7	−0.5	−0.8	−1.2	−1.1	−1.1

The PCC type of interactions occurs between the amino acid chains forming a parallel contact (P), where both contacting side chains are attached to a compact (C, most likely a helix) type of conformation

Table 3
Context pairwise contact potential for the PEE type of side chain interactions

PEE	GLY	ALA	SER	CYS	VAL	THR	ILE	PRO	MET	ASP	ASN	LEU	LYS	GLU	GLN	ARG	HIS	PHE	TYR	TRP
GLY	2.6	1.3	0.9	0.8	0.8	0.8	0.6	1.4	0.5	0.5	0.8	0.5	1.0	0.8	0.6	0.6	0.3	0.0	0.1	–0.2
ALA	1.3	0.5	0.5	–0.0	–0.4	0.2	–0.6	0.6	–0.2	0.6	0.3	–0.6	0.5	0.6	0.3	0.1	0.1	–0.8	–0.6	–0.8
SER	0.9	0.5	0.0	0.1	0.1	–0.3	–0.1	0.6	–0.1	–0.3	–0.3	0.0	–0.0	–0.2	–0.3	–0.3	–0.6	–0.4	–0.5	–0.7
CYS	0.8	–0.0	0.1	–0.8	–0.9	–0.0	–0.9	0.2	–0.7	0.3	0.3	–0.9	0.1	0.4	–0.1	0.0	–0.6	–0.9	–0.7	–1.5
VAL	0.8	–0.4	0.1	–0.9	–1.3	–0.5	–1.5	0.2	–0.9	0.3	0.0	–1.4	–0.2	–0.1	–0.1	–0.5	–0.6	–1.3	–1.1	–1.2
THR	0.8	0.2	–0.3	–0.0	–0.5	–0.7	–0.6	0.3	–0.4	–0.2	–0.5	–0.4	–0.5	–0.6	–0.6	–0.7	–0.7	–0.5	–0.6	–0.6
ILE	0.6	–0.6	–0.1	–0.9	–1.5	–0.6	–1.6	0.1	–1.1	0.1	–0.0	–1.5	–0.2	–0.2	–0.2	–0.5	–0.5	–1.5	–1.1	–1.3
PRO	1.4	0.6	0.6	0.2	0.2	0.3	0.1	1.0	0.2	0.8	0.4	0.1	0.8	0.6	0.3	0.1	0.0	–0.3	–0.5	–0.5
MET	0.5	–0.2	–0.1	–0.7	–0.9	–0.4	–1.1	0.2	–0.4	0.2	–0.1	–1.1	–0.2	–0.2	–0.5	–0.5	–0.5	–1.3	–0.9	–1.2
ASP	0.5	0.6	–0.3	0.3	0.3	–0.2	0.1	0.8	0.2	0.4	–0.5	0.2	–0.6	0.1	–0.5	–1.0	–0.7	0.0	–0.4	–0.4
ASN	0.8	0.3	–0.3	0.3	0.0	–0.5	–0.0	0.4	–0.1	–0.5	–0.5	0.1	–0.3	–0.4	–0.6	–0.5	–0.4	–0.3	–0.6	–0.6
LEU	0.5	–0.6	0.0	–0.9	–1.4	–0.4	–1.5	0.1	–1.1	0.2	0.1	–1.3	–0.1	–0.2	–0.3	–0.4	–0.5	–1.4	–1.1	–1.2
LYS	1.0	0.5	–0.0	0.1	–0.2	–0.5	–0.2	0.8	–0.2	–0.6	–0.3	–0.1	0.3	–1.1	–0.6	–0.1	–0.3	–0.3	–0.8	–1.0
GLU	0.8	0.6	–0.2	0.4	–0.1	–0.6	–0.2	0.6	–0.2	0.1	–0.4	–0.2	–1.1	0.4	–0.3	–1.3	–0.8	–0.3	–0.8	–0.7
GLN	0.6	0.3	–0.3	–0.1	–0.1	–0.6	–0.2	0.3	–0.5	–0.5	–0.6	–0.3	–0.6	–0.3	–0.3	–0.8	–0.6	–0.6	–0.8	–1.0
ARG	0.6	0.1	–0.3	0.0	–0.5	–0.7	–0.5	0.1	–0.5	–1.0	–0.5	–0.4	–0.1	–1.3	–0.8	–0.4	–0.7	–0.7	–1.0	–0.8
HIS	0.3	0.1	–0.6	–0.6	–0.6	–0.7	–0.5	0.0	–0.5	–0.7	–0.4	–0.5	–0.3	–0.8	–0.6	–0.7	–0.6	–0.6	–1.0	–0.7
PHE	0.0	–0.8	–0.4	–0.9	–1.3	–0.5	–1.5	–0.3	–1.3	0.0	–0.3	–1.4	–0.3	–0.3	–0.6	–0.7	–0.6	–1.4	–1.2	–1.4
TYR	0.1	–0.6	–0.5	–0.7	–1.1	–0.6	–1.1	–0.5	–0.9	–0.4	–0.6	–1.1	–0.8	–0.8	–0.8	–1.0	–1.0	–1.2	–0.9	–1.1
TRP	–0.2	–0.8	–0.7	–1.5	–1.2	–0.6	–1.3	–0.5	–1.2	–0.4	–0.6	–1.2	–1.0	–0.7	–1.0	–0.8	–0.7	–1.4	–1.1	–0.9

The PEE type of interactions occurs between the amino acid chains forming a parallel contact (P), where both contacting side chains are attached to expanded (E, most likely beta-strand) type of conformation

Table 4

Context pairwise contact potential for the PCE and the PEC type of side chain interactions

PCE/PEC	GLY	ALA	SER	CYS	VAL	THR	ILE	PRO	MET	ASP	ASN	LEU	LYS	GLU	GLN	ARG	HIS	PHE	TYR	TRP
GLY	3.3	2.5	1.4	1.5	1.3	0.9	1.2	2.2	0.8	0.8	1.1	1.3	0.9	1.0	0.9	0.7	1.1	1.0	0.6	0.6
ALA	2.3	1.4	0.8	0.7	1.1	0.9	1.0	1.5	0.8	0.4	0.3	1.0	1.3	1.3	1.2	0.9	0.9	0.6	0.5	0.4
SER	1.3	0.8	0.4	0.6	1.1	0.5	1.0	0.5	0.9	−0.5	0.3	0.9	0.5	0.4	0.2	0.1	0.5	0.6	0.6	0.5
CYS	0.8	0.6	0.5	−1.2	0.2	0.3	−0.1	0.7	0.0	0.8	0.2	0.0	0.6	1.0	0.5	−0.1	−0.2	−0.3	−0.0	−0.8
VAL	1.6	0.6	0.6	0.3	0.1	0.5	−0.0	0.7	0.0	0.1	0.2	−0.2	0.5	0.2	0.4	0.3	0.2	−0.0	0.0	0.2
THR	1.3	0.9	0.3	0.8	0.8	0.3	0.6	0.7	0.5	−0.3	0.0	0.6	0.1	0.1	0.3	0.1	0.2	0.5	0.1	0.4
ILE	1.3	0.5	0.4	0.2	0.1	0.3	−0.2	0.6	−0.2	0.6	0.2	−0.3	0.7	0.5	0.3	0.5	0.5	−0.4	−0.1	−0.2
PRO	1.6	1.4	1.3	1.4	0.9	1.0	0.8	1.2	1.1	1.0	0.4	0.8	1.0	0.7	0.6	0.7	0.8	0.3	−0.1	−0.1
MET	1.0	0.4	0.5	0.0	0.3	0.8	0.0	0.5	−0.1	0.4	0.1	−0.0	0.6	1.0	0.3	0.2	−0.1	−0.2	0.0	−0.4
ASP	1.0	1.1	0.1	1.1	1.2	0.1	1.2	0.8	0.8	0.2	−0.2	1.0	−0.2	0.8	0.3	−0.5	−0.1	1.0	0.2	0.6
ASN	1.3	1.2	0.5	1.2	0.9	0.3	1.1	0.9	0.7	−0.2	−0.2	0.8	0.3	0.3	0.2	0.0	0.2	0.9	0.1	0.2
LEU	1.3	0.5	0.6	0.1	−0.0	0.6	−0.3	0.8	−0.0	0.6	0.4	−0.4	0.7	0.7	0.5	0.3	0.1	−0.3	−0.2	−0.4
LYS	1.8	1.9	0.6	1.6	1.3	0.4	1.3	1.0	0.8	−0.2	0.2	1.1	1.1	−0.1	0.5	0.7	0.5	0.8	0.4	0.4
GLU	1.3	1.3	0.1	1.1	1.6	0.2	1.3	0.7	0.9	0.5	0.1	1.3	−0.1	0.9	0.6	−0.3	0.2	1.0	0.7	0.4
GLN	1.0	1.1	0.4	1.3	1.4	0.5	0.8	0.7	0.6	0.1	0.3	0.8	0.4	0.5	0.3	0.1	0.6	0.6	0.5	−0.1
ARG	1.1	1.2	0.5	0.6	1.0	0.5	0.8	0.4	1.0	−0.5	0.1	0.7	0.5	−0.1	0.1	0.4	0.2	0.5	0.1	0.4
HIS	1.3	0.8	0.2	−0.1	0.6	0.2	0.5	0.3	0.6	0.0	−0.0	0.6	0.1	0.0	0.1	0.2	−0.1	0.1	−0.2	−0.4
PHE	1.0	0.2	0.2	−0.3	−0.2	0.1	−0.4	0.6	−0.5	0.3	0.0	−0.4	0.6	0.4	0.3	0.1	−0.1	−0.7	−0.4	−0.3
TYR	1.0	0.6	0.2	0.2	0.2	0.1	−0.0	−0.1	−0.2	0.0	−0.2	−0.1	0.2	0.2	0.3	−0.1	−0.4	−0.4	−0.1	−0.5
TRP	0.7	0.0	0.0	−0.1	−0.0	−0.2	−0.5	−0.4	−0.6	0.2	−0.1	−0.3	0.2	−0.2	−0.3	0.1	−0.3	−0.7	−0.4	−0.4

The PCE type of interactions occurs between amino acid chains forming a parallel contact (P), where the first contacting side chain (given in columns) is attached to the compact (C, most likely a helix) type of conformation and the second contacting side chain (given in rows) is attached to expanded (E, most likely beta-strand) conformation

Table 5
Context pairwise contact potential for the MCC type of side chain interactions

MCC	GLY	ALA	SER	CYS	VAL	THR	ILE	PRO	MET	ASP	ASN	LEU	LYS	GLU	GLN	ARG	HIS	PHE	TYR	TRP
GLY	2.0	1.4	1.1	0.7	1.0	1.0	0.7	1.2	0.5	0.9	0.9	0.7	1.0	1.3	0.8	0.5	1.0	0.4	0.4	0.2
ALA	1.4	0.3	0.4	0.0	–0.2	0.0	–0.3	0.5	–0.3	0.5	0.5	–0.3	0.4	0.3	0.3	0.1	0.4	–0.4	–0.4	–0.5
SER	1.1	0.4	0.6	0.4	0.1	0.2	0.2	0.5	0.2	0.3	0.4	0.1	0.2	0.5	0.1	0.1	0.1	–0.1	–0.1	–0.2
CYS	0.7	0.0	0.4	–1.3	–0.3	0.2	–0.5	0.3	–0.7	0.6	0.5	–0.5	0.5	0.5	0.8	0.1	–0.6	–0.9	–0.6	–0.9
VAL	1.0	–0.2	0.1	–0.3	–0.5	–0.1	–0.8	–0.0	–0.8	0.5	0.5	–0.8	0.5	0.2	0.1	0.1	–0.1	–0.8	–0.7	–1.1
THR	1.0	0.0	0.2	0.2	–0.1	0.2	–0.2	0.2	–0.3	0.3	0.0	–0.2	0.2	0.3	0.0	–0.0	0.0	–0.3	–0.3	–0.6
ILE	0.7	–0.3	0.2	–0.5	–0.8	–0.2	-0.8	0.1	–1.0	0.5	0.3	–1.0	0.2	0.1	0.0	–0.2	–0.2	–1.1	–0.9	–1.2
PRO	1.2	0.5	0.5	0.3	–0.0	0.2	0.1	0.7	0.0	0.6	0.5	0.2	0.5	0.7	0.3	–0.0	0.2	–0.3	–0.3	–0.3
MET	0.5	–0.3	0.2	–0.7	–0.8	–0.3	–1.0	0.0	–0.6	0.4	0.3	–0.9	0.2	0.3	–0.1	–0.3	–0.4	–1.1	–0.9	–1.2
ASP	0.9	0.5	0.3	0.6	0.5	0.3	0.5	0.6	0.4	0.5	0.2	0.6	–0.3	0.4	0.4	–0.6	–0.1	0.3	–0.2	–0.1
ASN	0.9	0.5	0.4	0.5	0.5	0.0	0.3	0.5	0.3	0.2	0.3	0.4	0.1	0.2	0.2	–0.1	0.1	0.1	–0.3	–0.4
LEU	0.7	–0.3	0.1	–0.5	–0.8	–0.2	–1.0	0.2	–0.9	0.6	0.4	–1.1	0.2	0.2	–0.1	–0.1	–0.2	–1.2	–0.9	–1.3
LYS	1.0	0.4	0.2	0.5	0.5	0.2	0.2	0.5	0.2	–0.3	0.1	0.2	0.9	–0.4	0.0	0.3	0.4	0.1	–0.3	–0.1
GLU	1.3	0.3	0.5	0.5	0.2	0.3	0.1	0.7	0.3	0.4	0.2	0.2	–0.4	0.4	0.0	–0.6	–0.2	0.0	–0.4	–0.2
GLN	0.8	0.3	0.1	0.8	0.1	0.0	0.0	0.3	–0.1	0.4	0.2	–0.1	0.0	0.0	0.1	–0.1	0.0	–0.1	–0.3	–0.5
ARG	0.5	0.1	0.1	0.1	0.1	–0.0	–0.2	–0.0	–0.3	–0.6	–0.1	–0.1	0.3	–0.6	–0.1	0.1	–0.0	–0.3	–0.6	–0.6
HIS	1.0	0.4	0.1	–0.6	–0.1	0.0	–0.2	0.2	–0.4	–0.1	0.1	–0.2	0.4	–0.2	0.0	–0.0	–0.0	–0.3	–0.3	–1.0
PHE	0.4	–0.4	–0.1	–0.9	–0.8	–0.3	–1.1	–0.3	–1.1	0.3	0.1	–1.2	0.1	0.0	–0.1	–0.3	–0.3	–1.2	–1.2	–1.5
TYR	0.4	–0.4	–0.1	–0.6	–0.7	–0.3	–0.9	–0.3	–0.9	–0.2	–0.3	–0.9	–0.3	–0.4	–0.3	–0.6	–0.3	–1.2	–0.7	–1.3
TRP	0.2	–0.5	–0.2	–0.9	–1.1	–0.6	–1.2	–0.3	–1.2	–0.1	–0.4	–1.3	–0.1	–0.2	–0.5	–0.6	–1.0	–1.5	–1.3	–1.2

The MCC type of interactions occurs between the amino acid chains forming a medium-intermediate contact (M), where both contacting side chains are attached to a compact (C, most likely a helix) type of conformation

Table 6
Context pairwise contact potential for the MEE type of side chain interactions

MEE	GLY	ALA	SER	CYS	VAL	THR	ILE	PRO	MET	ASP	ASN	LEU	LYS	GLU	GLN	ARG	HIS	PHE	TYR	TRP
GLY	1.5	1.2	0.8	0.2	0.6	0.5	0.6	0.8	0.3	0.7	0.3	0.5	0.9	0.7	0.7	0.3	0.1	–0.0	–0.3	–0.5
ALA	1.2	0.4	0.5	–0.3	–0.3	0.2	–0.4	0.3	–0.2	0.5	0.3	–0.2	0.5	0.4	0.4	0.1	0.1	–0.5	–0.4	–0.8
SER	0.8	0.5	0.4	0.0	0.1	0.1	0.1	0.4	0.2	0.1	–0.1	0.2	0.4	0.1	0.1	0.0	–0.2	–0.1	–0.3	–0.4
CYS	0.2	–0.3	0.0	–1.4	–0.5	–0.2	–0.5	–0.1	–0.5	0.3	0.2	–0.6	0.3	0.6	–0.0	–0.1	–0.5	–0.8	–0.8	–1.0
VAL	0.6	–0.3	0.1	–0.5	–0.4	0.1	–0.6	–0.1	–0.5	0.5	0.3	–0.7	0.2	0.4	0.0	–0.0	–0.1	–0.9	–0.7	–1.1
THR	0.5	0.2	0.1	–0.2	0.1	0.2	–0.0	0.1	0.1	–0.0	0.1	0.0	0.2	0.1	0.1	–0.2	–0.0	–0.2	–0.3	–0.4
ILE	0.6	–0.4	0.1	–0.5	–0.6	–0.0	–0.8	–0.2	–0.6	0.4	0.3	–0.8	0.3	0.4	0.1	0.0	–0.2	–1.0	–0.8	–1.1
PRO	0.8	0.3	0.4	–0.1	–0.1	0.1	–0.2	0.5	–0.3	0.6	0.2	–0.0	0.3	0.3	0.0	0.0	0.1	–0.3	–0.8	–0.9
MET	0.3	–0.2	0.2	–0.5	–0.5	0.1	–0.6	–0.3	–0.3	0.1	–0.2	–0.8	0.0	0.2	–0.1	–0.3	–0.2	–0.9	–0.7	–1.2
ASP	0.7	0.5	0.1	0.3	0.5	–0.0	0.4	0.6	0.1	0.3	–0.3	0.4	–0.3	0.4	0.1	–0.5	–0.5	0.1	–0.5	–0.4
ASN	0.3	0.3	–0.1	0.2	0.3	0.1	0.3	0.2	–0.2	–0.3	–0.1	0.2	0.2	0.0	0.2	–0.1	–0.2	–0.1	–0.4	–0.6
LEU	0.5	–0.2	0.2	–0.6	–0.7	0.0	–0.8	–0.0	–0.8	0.4	0.2	–0.8	0.2	0.4	0.0	–0.1	–0.1	–1.1	–0.8	–1.2
LYS	0.9	0.5	0.4	0.3	0.2	0.2	0.3	0.3	0.0	–0.3	0.2	0.2	0.8	–0.4	0.0	0.2	0.2	–0.1	–0.5	–0.6
GLU	0.7	0.4	0.1	0.6	0.4	0.1	0.4	0.3	0.2	0.4	0.0	0.4	–0.4	0.6	0.0	–0.7	–0.3	0.0	–0.4	–0.6
GLN	0.7	0.4	0.1	–0.0	0.0	0.1	0.1	0.0	–0.1	0.1	0.2	0.0	0.0	0.0	0.1	–0.3	–0.3	–0.4	–0.6	–0.7
ARG	0.3	0.1	0.0	–0.1	–0.0	–0.2	0.0	0.0	–0.3	–0.5	–0.1	–0.1	0.2	–0.7	–0.3	0.1	–0.2	–0.4	–0.8	–1.1
HIS	0.1	0.1	–0.2	–0.5	–0.1	–0.0	–0.2	0.1	–0.2	–0.5	–0.2	–0.1	0.2	–0.3	–0.3	–0.2	–0.7	–0.5	–0.8	–0.8
PHE	–0.0	–0.5	–0.1	–0.8	–0.9	–0.2	–1.0	–0.3	–0.9	0.1	–0.1	–1.1	–0.1	0.0	–0.4	–0.4	–0.5	–1.2	–1.1	–1.5
TYR	–0.3	–0.4	–0.3	–0.8	–0.7	–0.3	–0.8	–0.8	–0.7	–0.5	–0.4	–0.8	–0.5	–0.4	–0.6	–0.8	–0.8	–1.1	–0.6	–1.5
TRP	–0.5	–0.8	–0.4	–1.0	–1.1	–0.4	–1.1	–0.9	–1.2	–0.4	–0.6	–1.2	–0.6	–0.6	–0.7	–1.1	–0.8	–1.5	–1.5	–1.2

The MEE type of interactions occurs between the amino acid chains forming a medium-intermediate contact (M), where both contacting side chains are attached to expanded (E, most likely beta-strand) type of conformation

Table 7
Context pairwise contact potential for the MCE and the MEC type of side chain interactions

MCE/MEC	GLY	ALA	SER	CYS	VAL	THR	ILE	PRO	MET	ASP	ASN	LEU	LYS	GLU	GLN	ARG	HIS	PHE	TYR	TRP
GLY	2.0	1.3	1.0	0.9	1.3	0.9	1.1	1.3	0.9	0.6	0.6	0.9	1.2	1.4	0.9	0.6	1.0	0.5	0.5	0.7
ALA	1.5	0.9	0.5	0.5	0.4	0.4	0.2	0.8	0.1	0.5	0.6	0.1	1.0	1.1	1.0	0.7	0.7	−0.0	0.2	−0.1
SER	1.0	1.0	0.4	0.5	0.7	0.5	0.7	0.5	0.4	−0.1	0.1	0.6	0.5	0.5	0.7	0.4	0.1	0.2	0.1	0.2
CYS	0.6	0.2	0.2	−1.7	−0.2	0.1	−0.6	−0.0	−0.5	0.2	0.3	−0.4	0.4	0.7	0.1	−0.1	−0.5	−0.6	−0.3	−0.6
VAL	0.7	0.2	0.3	−0.1	−0.4	0.3	−0.5	0.0	−0.5	0.4	0.3	−0.7	0.7	0.5	0.3	0.2	0.1	−0.8	−0.4	−0.6
THR	0.8	0.5	0.2	0.3	0.2	0.3	0.2	0.1	0.0	−0.3	−0.1	−0.0	0.4	0.5	0.3	0.3	0.1	−0.1	0.0	−0.3
ILE	0.7	−0.1	0.5	−0.2	−0.6	−0.0	−1.0	−0.1	−0.5	0.5	0.2	−0.8	0.7	0.5	0.3	0.1	0.2	−0.9	−0.6	−0.8
PRO	1.0	0.7	0.7	0.3	0.4	0.8	0.3	0.5	0.3	0.6	0.2	0.4	0.7	0.7	0.5	0.1	0.1	0.1	−0.4	−0.6
MET	0.6	−0.0	0.5	−0.1	−0.5	0.1	−0.8	0.1	−0.4	0.3	−0.2	−0.7	0.8	1.0	0.2	0.1	0.0	−0.9	−0.8	−0.8
ASP	0.7	0.7	−0.2	0.5	0.7	−0.1	0.6	0.3	0.2	0.0	−0.1	0.2	−0.4	0.6	0.2	−0.7	−0.2	0.2	−0.3	−0.1
ASN	0.7	0.6	0.3	0.8	0.6	0.3	0.6	0.2	0.3	−0.3	−0.2	0.5	0.3	0.3	0.1	−0.2	0.2	0.2	−0.1	−0.5
LEU	0.9	0.0	0.5	−0.2	−0.6	0.2	−0.9	0.0	−0.7	0.7	0.5	−0.9	0.7	0.8	0.4	0.3	0.1	−1.0	−0.6	−0.8
LYS	1.2	1.0	0.7	0.8	0.9	0.6	0.7	0.9	0.5	−0.0	0.2	0.5	1.1	0.3	0.7	0.7	0.6	0.3	−0.1	0.1
GLU	1.0	1.0	−0.1	0.7	0.8	−0.2	0.6	0.4	0.1	0.4	0.0	0.4	−0.0	1.0	0.4	−0.3	0.1	0.2	0.1	−0.1
GLN	0.8	0.5	0.1	0.3	0.6	−0.2	0.4	0.3	−0.0	0.0	−0.1	0.1	0.3	0.4	0.4	−0.0	0.3	0.1	−0.3	−0.3
ARG	0.9	0.6	0.3	0.4	0.6	0.1	0.2	0.1	0.0	−0.3	0.1	0.2	0.7	−0.1	0.0	0.1	0.1	−0.1	−0.1	−0.3
HIS	0.6	0.5	−0.0	−0.7	0.2	−0.1	−0.0	0.1	−0.2	−0.5	0.1	−0.1	0.4	0.2	0.1	−0.1	−0.8	−0.4	−0.4	−0.7
PHE	0.4	−0.1	−0.0	−0.7	−0.7	−0.1	−1.0	−0.2	−1.1	0.1	−0.1	−1.0	0.4	0.2	−0.1	−0.2	−0.2	−1.2	−0.8	−1.2
TYR	0.2	0.2	−0.1	−0.2	−0.4	−0.2	−0.7	−0.6	−0.6	−0.4	−0.1	−0.7	−0.1	−0.0	0.1	−0.5	−0.6	−0.9	−0.8	−1.0
TRP	0.0	−0.6	−0.3	−0.6	−0.8	−0.3	−0.9	−0.9	−1.2	−0.0	−0.3	−1.2	−0.0	−0.0	−0.5	−0.7	−0.6	−1.3	−0.9	−1.1

The MCE type of interactions occurs between amino acid chains forming a medium-intermediate contact (M), where the first contacting side chain (given in columns) is attached to the compact (C, most likely a helix) type of conformation and the second contacting side chain (given in rows) is attached to expanded (E, most likely beta-strand) conformation

Table 8
Context pairwise contact potential for the ACC type of side chain interactions

ACC	GLY	ALA	SER	CYS	VAL	THR	ILE	PRO	MET	ASP	ASN	LEU	LYS	GLU	GLN	ARG	HIS	PHE	TYR	TRP
GLY	1.5	0.8	1.1	0.1	0.6	0.8	0.5	0.9	0.4	1.3	1.0	0.6	1.3	1.5	1.1	1.0	0.9	0.2	0.2	0.1
ALA	0.8	0.0	0.6	−0.4	−0.6	0.2	−0.7	0.3	−0.4	1.4	0.9	−0.5	0.9	1.1	0.8	0.6	0.3	−0.6	−0.6	−0.4
SER	1.1	0.6	0.8	0.1	0.1	0.8	−0.0	0.4	−0.0	1.1	0.8	0.1	1.0	1.4	1.0	0.7	0.7	0.1	0.1	−0.3
CYS	0.1	−0.4	0.1	−1.9	−0.8	−0.2	−0.5	−0.5	−0.9	0.9	0.5	−0.7	0.6	0.4	0.2	0.1	−0.4	−1.0	−0.8	−0.8
VAL	0.6	−0.6	0.1	−0.8	−0.8	−0.2	−1.3	−0.2	−0.8	0.7	0.4	−1.2	0.3	0.5	0.2	−0.2	−0.1	−1.2	−1.0	−1.1
THR	0.8	0.2	0.8	−0.2	−0.2	0.5	−0.4	0.2	−0.2	1.2	0.6	−0.3	1.3	0.9	0.7	0.3	0.1	−0.3	−0.3	−0.5
ILE	0.5	−0.7	−0.0	−0.5	−1.3	−0.4	−1.3	−0.2	−1.0	0.7	0.5	−1.3	0.2	0.3	0.0	−0.2	−0.4	−1.4	−1.2	−1.4
PRO	0.9	0.3	0.4	−0.5	−0.2	0.2	−0.2	0.6	−0.1	0.7	0.5	−0.2	0.7	0.7	0.5	0.2	0.1	−0.5	−0.5	−0.8
MET	0.4	−0.4	−0.0	−0.9	−0.8	−0.2	−1.0	−0.1	−1.1	0.8	0.3	−1.1	0.6	0.7	0.2	−0.1	−0.3	−1.4	−1.2	−1.3
ASP	1.3	1.4	1.1	0.9	0.7	1.2	0.7	0.7	0.8	2.1	1.3	0.9	0.8	2.0	1.4	0.3	0.3	0.4	−0.0	0.0
ASN	1.0	0.9	0.8	0.5	0.4	0.6	0.5	0.5	0.3	1.3	1.0	0.5	1.0	1.3	1.0	0.6	0.8	0.1	−0.2	−0.2
LEU	0.6	−0.5	0.1	−0.7	−1.2	−0.3	−1.3	−0.2	−1.1	0.9	0.5	−1.3	0.1	0.5	−0.0	−0.2	−0.3	−1.4	−1.2	−1.2
LYS	1.3	0.9	1.0	0.6	0.3	1.3	0.2	0.7	0.6	0.8	1.0	0.1	2.2	1.0	1.2	1.4	1.0	0.1	0.0	−0.2
GLU	1.5	1.1	1.4	0.4	0.5	0.9	0.3	0.7	0.7	2.0	1.3	0.5	1.0	1.8	1.3	0.5	0.2	0.3	0.1	−0.1
GLN	1.1	0.8	1.0	0.2	0.2	0.7	0.0	0.5	0.2	1.4	1.0	−0.0	1.2	1.3	0.9	0.7	0.9	−0.2	−0.0	−0.6
ARG	1.0	0.6	0.7	0.1	−0.2	0.3	−0.2	0.2	−0.1	0.3	0.6	−0.2	1.4	0.5	0.7	1.2	0.4	−0.4	−0.3	−0.5
HIS	0.9	0.3	0.7	−0.4	−0.1	0.1	−0.4	0.1	−0.3	0.3	0.8	−0.3	1.0	0.2	0.9	0.4	−0.3	−0.6	−0.6	−0.4
PHE	0.2	−0.6	0.1	−1.0	−1.2	−0.3	−1.4	−0.5	−1.4	0.4	0.1	−1.4	0.1	0.3	−0.2	−0.4	−0.6	−1.4	−1.4	−1.5
TYR	0.2	−0.6	0.1	−0.8	−1.0	−0.3	−1.2	−0.5	−1.2	−0.0	−0.2	−1.2	0.0	0.1	−0.0	−0.3	−0.6	−1.4	−0.9	−1.1
TRP	0.1	−0.4	−0.3	−0.8	−1.1	−0.5	−1.4	−0.8	−1.3	0.0	−0.2	−1.2	−0.2	−0.1	−0.6	−0.5	−0.4	−1.5	−1.1	−0.8

The ACC type of interactions occurs between the amino acid chains forming an antiparallel contact (A), where both contacting side chains are attached to a compact (C, most likely a helix) type of conformation

Table 9
Context pairwise contact potential for the AEE type of side chain interactions

AEE	GLY	ALA	SER	CYS	VAL	THR	ILE	PRO	MET	ASP	ASN	LEU	LYS	GLU	GLN	ARG	HIS	PHE	TYR	TRP
GLY	1.0	0.9	0.6	0.3	0.6	0.5	0.4	0.8	0.5	0.6	0.5	0.3	1.4	1.0	0.8	0.7	0.6	–0.2	0.1	0.2
ALA	0.9	0.9	0.9	0.3	–0.0	0.8	–0.3	0.4	–0.2	1.0	0.6	–0.2	0.9	1.2	0.4	0.7	0.5	–0.5	–0.3	–0.4
SER	0.6	0.9	1.0	0.3	0.5	0.7	0.4	0.5	0.6	0.8	0.5	0.3	1.0	0.9	0.6	0.4	0.4	0.1	–0.0	–0.4
CYS	0.3	0.3	0.3	–2.4	–0.1	0.1	–0.5	0.3	–0.5	0.4	0.1	–0.7	0.5	0.6	0.0	0.1	–0.4	–0.8	–0.6	–1.4
VAL	0.6	–0.0	0.5	–0.1	–0.5	0.4	–0.7	0.2	–0.6	1.1	0.8	–0.8	0.6	0.7	0.4	0.3	0.0	–1.0	–0.5	–1.3
THR	0.5	0.8	0.7	0.1	0.4	0.7	0.2	0.7	0.2	0.9	0.3	0.2	1.1	1.0	0.6	0.4	0.2	–0.1	–0.1	–0.5
ILE	0.4	–0.3	0.4	–0.5	–0.7	0.2	–0.9	0.1	–0.8	0.6	0.4	–1.1	0.4	0.7	0.2	0.2	0.1	–1.3	–0.9	–1.3
PRO	0.8	0.4	0.5	0.3	0.2	0.7	0.1	0.3	0.1	0.5	0.3	0.1	1.2	0.6	0.4	0.4	0.2	–0.2	–0.4	–0.9
MET	0.5	–0.2	0.6	–0.5	–0.6	0.2	–0.8	0.1	0.1	0.4	0.1	–0.8	0.5	0.3	0.4	0.3	–0.3	–1.0	–0.8	–0.8
ASP	0.6	1.0	0.8	0.4	1.1	0.9	0.6	0.5	0.4	1.2	0.4	0.7	0.5	1.2	0.5	0.3	–0.0	0.7	0.2	0.2
ASN	0.5	0.6	0.5	0.1	0.8	0.3	0.4	0.3	0.1	0.4	0.6	0.4	1.2	0.9	0.3	0.4	–0.3	0.2	0.1	–0.5
LEU	0.3	–0.2	0.3	–0.7	–0.8	0.2	–1.1	0.1	–0.8	0.7	0.4	–0.9	0.2	0.7	0.3	0.0	–0.2	–1.2	–1.1	–1.6
LYS	1.4	0.9	1.0	0.5	0.6	1.1	0.4	1.2	0.5	0.5	1.2	0.2	1.7	0.8	0.6	1.0	0.6	0.4	0.1	0.4
GLU	1.0	1.2	0.9	0.6	0.7	1.0	0.7	0.6	0.3	1.2	0.9	0.7	0.8	1.7	0.8	0.3	0.5	0.4	0.1	–0.2
GLN	0.8	0.4	0.6	0.0	0.4	0.6	0.2	0.4	0.4	0.5	0.3	0.3	0.6	0.8	1.2	0.6	0.6	–0.2	–0.1	–0.4
ARG	0.7	0.7	0.4	0.1	0.3	0.4	0.2	0.4	0.3	0.3	0.4	0.0	1.0	0.3	0.6	1.0	0.4	–0.2	–0.3	–0.4
HIS	0.6	0.5	0.4	–0.4	0.0	0.2	0.1	0.2	–0.3	–0.0	–0.3	–0.2	0.6	0.5	0.6	0.4	–0.2	–0.5	–0.4	–0.9
PHE	–0.2	–0.5	0.1	–0.8	–1.0	–0.1	–1.3	–0.2	–1.0	0.7	0.2	–1.2	0.4	0.4	–0.2	–0.2	–0.5	–1.2	–1.0	–1.5
TYR	0.1	–0.3	–0.0	–0.6	–0.5	–0.1	–0.9	–0.4	–0.8	0.2	0.1	–1.1	0.1	0.1	–0.1	–0.3	–0.4	–1.0	–0.7	–1.1
TRP	0.2	–0.4	–0.4	–1.4	–1.3	–0.5	–1.3	–0.9	–0.8	0.2	–0.5	–1.6	0.4	–0.2	–0.4	–0.4	–0.9	–1.5	–1.1	–0.8

The AEE type of interactions occurs between the amino acid chains forming an antiparallel contact (A), where both contacting side chains are attached to expanded (E, most likely beta-strand) type of conformation

Table 10
Context pairwise contact potential for the ACE and the AEC type of side chain interactions

ACE/AEC	GLY	ALA	SER	CYS	VAL	THR	ILE	PRO	MET	ASP	ASN	LEU	LYS	GLU	GLN	ARG	HIS	PHE	TYR	TRP
GLY	1.2	1.2	1.0	0.7	0.7	0.6	0.7	1.1	0.5	0.1	0.1	0.7	1.7	1.5	1.1	0.8	0.9	0.5	0.3	**0.6**
ALA	1.0	0.0	0.9	–0.2	–0.6	0.6	–0.8	0.6	–0.5	1.0	0.9	–0.5	1.2	1.3	0.8	0.6	0.3	–0.7	–0.6	**–0.6**
SER	1.1	0.9	0.7	0.3	0.2	0.8	0.3	0.7	0.3	0.7	0.6	0.1	0.9	1.3	0.6	0.4	0.4	–0.0	–0.2	**0.0**
CYS	0.3	–0.3	0.4	–2.6	–0.8	–0.2	–0.9	–0.4	–0.9	0.5	0.2	–0.9	0.1	1.1	0.4	–0.1	–0.5	–1.3	–1.1	**–1.4**
VAL	0.4	–0.3	0.4	–0.5	–1.1	0.2	–1.3	0.0	–0.7	0.6	0.5	–1.1	0.8	0.5	0.3	–0.0	–0.2	–1.3	–1.0	**–1.2**
THR	0.8	0.3	0.5	–0.3	–0.1	0.7	–0.4	0.3	–0.3	0.8	0.3	–0.3	0.8	0.8	0.6	0.4	–0.2	–0.5	–0.5	**–0.6**
ILE	0.4	–0.5	0.7	–0.4	–1.1	0.0	–1.5	–0.2	–1.0	0.8	0.4	–1.3	0.5	0.5	0.1	–0.1	–0.2	–1.4	–1.2	**–1.3**
PRO	1.0	0.7	0.7	0.3	0.3	0.7	0.2	0.4	0.3	1.1	0.6	0.2	1.2	0.8	0.5	0.5	–0.2	–0.0	–0.4	**–0.8**
MET	0.2	–0.7	0.4	–0.5	–0.8	–0.2	–1.2	–0.1	–0.9	0.5	–0.0	–1.2	0.9	1.0	0.8	–0.2	0.0	–1.4	–1.0	**–1.3**
ASP	1.3	0.8	0.8	0.9	1.0	1.2	0.4	1.0	0.9	1.6	0.7	0.8	0.5	1.9	1.3	0.3	0.3	0.5	–0.2	**0.0**
ASN	0.9	0.7	0.7	0.3	0.6	0.4	0.3	0.4	0.4	0.7	0.5	0.3	1.1	1.1	0.8	0.4	0.4	–0.0	0.1	**–0.2**
LEU	0.5	–0.5	0.3	–0.6	–1.2	0.1	–1.4	–0.2	–0.8	1.1	0.5	–1.3	0.5	0.7	0.3	–0.0	–0.4	–1.4	–1.2	**–1.2**
LYS	1.2	1.0	1.0	0.7	0.3	0.9	–0.0	0.8	0.1	0.7	1.1	0.1	1.5	0.9	0.8	1.7	0.9	–0.2	–0.1	**–0.3**
GLU	1.3	1.0	0.9	0.6	0.4	0.8	0.2	0.9	0.5	1.8	0.9	0.3	0.8	1.6	1.6	0.3	0.5	–0.0	–0.2	**0.1**
GLN	0.7	0.7	0.7	0.1	0.1	0.6	–0.2	0.3	0.3	0.9	0.5	–0.1	1.3	1.1	1.2	0.7	0.3	–0.3	–0.4	**–0.7**
ARG	1.0	0.6	0.7	–0.0	0.1	0.2	–0.2	0.2	0.1	0.0	0.6	–0.3	1.2	0.1	0.4	0.7	0.4	–0.5	–0.5	**–0.6**
HIS	0.9	–0.0	0.3	–0.9	–0.2	0.3	–0.2	0.2	–0.1	0.2	–0.1	–0.1	1.0	0.3	1.2	0.3	–0.4	–0.7	–0.7	**–0.1**
PHE	0.3	–0.5	0.1	–0.7	–1.2	–0.2	–1.4	–0.3	–1.1	0.4	0.5	–1.3	0.1	0.4	–0.2	–0.3	–0.6	–1.7	–1.2	**–1.4**
TYR	0.4	–0.1	0.5	–0.3	–0.7	–0.1	–0.9	–0.5	–1.0	–0.0	–0.0	–0.9	0.2	0.1	–0.5	–0.5	–0.4	–1.2	–0.8	**–1.1**
TRP	–0.1	–0.5	0.0	–0.9	–1.0	–0.3	–1.3	–1.0	–1.3	0.2	–0.3	–1.2	0.1	0.1	0.0	–0.7	–0.9	–1.5	–1.2	**–1.3**

The ACE type of interactions occurs between amino acid chains forming an antiparallel contact (A), where the first contacting side chain (given in columns) is attached to the compact (C, most likely a helix) type of conformation and the second contacting side chain (given in rows) is attached to expanded (E, most likely beta-strand) conformation

2. The basic output of the CABS model is a trajectory in Cα representation. The CABS coarse-grained trajectories, or selected trajectory models, can be reconstructed to all-atom representation. The major output of the CABS-based multiscale methods (like CABS-fold or CABS-dock servers) is a set of a few models in all-atom representation (automatically selected and reconstructed). These methods also provide hundreds (CABS-fold) or thousands (CABS-dock) of predicted models in Cα trajectories that may be useful in a more thorough analysis of the prediction results and reconstructed to all-atom resolution by the user.

   There are many strategies for the reconstruction from the Cα to all-atom format; however, the method chosen should be insensitive to small local distortions of the C-alpha distances present in CABS-generated models. Based on our experience, we can recommend the following reconstruction protocols:

   - ModRefiner package [40] for combined reconstruction and optimization (handles only monomeric protein chains, employed in the CABS-fold [14] server).
   - Modeller package [41] for combined reconstruction and optimization (employed in the CABS-dock server, details of the Modeller protocol are provided in ref. [16] and the CABS-dock online tutorial http://biocomp.chem.uw.edu.pl/CABSdock/tutorial).
   - Claessens et al. [42] or BBQ [43] approach for protein backbone reconstruction followed by the second rebuilding step (side chain reconstruction) using the SCWRL program [44].
   - The last two-step protocols require a third additional optimization step, which is more demanding when BBQ is used for backbone reconstruction [45]. We tested the performance of such reconstruction and fast optimization protocols in protein structure prediction [45] and protein dynamics [30] exercises. Optimization strategies have also been reviewed in ref. [46].

3. Reconstructed and optimized all-atom models can be assessed using specially designed scoring methods. An accurate scoring function that can discriminate near-native models, or docking poses, from a large set of alternative solutions is an important component of structure prediction methodologies [47–49].
4. CABS modeling trajectories can be additionally analyzed using external tools for the structural clustering and comparison of protein models, e.g., the ClusCo package [50] or hierarchical clustering within the Bioshell package [51]. Convenient analysis of protein models usually requires superimposition of the compared models, or entire trajectories; a useful tool for that is the Theseus package [52].

5. The accuracy of de novo structure prediction by CABS-fold or CABS-dock servers depends on the accuracy of the secondary structure input. Small errors in the predicted secondary structure do not impose any serious problems, but it is (on average) safer to use underestimated ranges of regular (helices and beta strands) secondary structure fragments than overestimated ranges (for instance prediction of a single long helix for the fragment that forms two differently oriented helices). Qualitative errors of secondary structure predictions, where helical fragments are predicted as beta strands (or vice versa), are dangerous for modeling results. Fortunately, this kind of errors is rare for good bioinformatics tools for secondary structure prediction and could be eliminated by rejecting more problematic predictions.

Acknowledgments

Funding for this work was provided by the National Science Center grant [MAESTRO 2014/14/A/ST6/0008] and by the Foundation for Polish Science TEAM project (TEAM/2011-7/6) cofinanced by the EU European Regional Development Fund operated within the Innovative Economy Operational Program.

References

1. Lindorff-Larsen K, Piana S, Dror RO, Shaw DE (2011) How fast-folding proteins fold. Science 334:517–520
2. Kmiecik S, Wabik J, Kolinski M, Kouza M, Kolinski A (2014) Coarse-grained modeling of protein dynamics. In: Computational methods to study the structure and dynamics of biomolecules and biomolecular processes, vol 1, Springer, Heidelberg, Berlin, pp 55–79
3. Kmiecik S, Gront D, Kolinski M, Wieteska L, Dawid AE, Kolinski A (2016) Coarse-grained protein models and their applications. Chem Rev. doi: 10.1021/acs.chemrev.6b00163
4. Kmiecik S, Jamroz M, Kolinski A (2011) Multiscale approach to protein folding dynamics. In: Multiscale approaches to protein modeling. Springer, New York, pp 281–293
5. Levitt M, Warshel A (1975) Computer simulation of protein folding. Nature 253:694–698
6. Rohl CA, Strauss CEM, Misura KMS, Baker D (2004) Protein structure prediction using Rosetta. In: Methods Enzymol, vol 383, Academic Press, pp 66–93
7. Mao B, Tejero R, Baker D, Montelione GT (2014) Protein NMR structures refined with Rosetta have higher accuracy relative to corresponding X-ray crystal structures. J Am Chem Soc 136:1893–1906
8. Roy A, Kucukural A, Zhang Y (2010) I-TASSER: a unified platform for automated protein structure and function prediction. Nat Protoc 5:725–738
9. Yang J, Yan R, Roy A, Xu D, Poisson J, Zhang Y (2015) The I-TASSER suite: protein structure and function prediction. Nat Methods 12:7–8
10. Kolinski A (2004) Protein modeling and structure prediction with a reduced representation. Acta Biochim Pol 51:349–371
11. Kmiecik S, Kolinski A (2007) Characterization of protein-folding pathways by reduced-space modeling. Proc Natl Acad Sci U S A 104: 12330–12335
12. Liwo A, Khalili M, Scheraga HA (2005) Ab initio simulations of protein-folding pathways by molecular dynamics with the united-residue

model of polypeptide chains. Proc Natl Acad Sci U S A 102:2362–2367

13. Liwo A, He Y, Scheraga HA (2011) Coarse-grained force field: general folding theory. Phys Chem Chem Phys 13:16890–16901
14. Blaszczyk M, Jamroz M, Kmiecik S, Kolinski A (2013) CABS-fold: server for the de novo and consensus-based prediction of protein structure. Nucleic Acids Res 41:W406–W411
15. Kurcinski M, Jamroz M, Blaszczyk M, Kolinski A, Kmiecik S (2015) CABS-dock web server for the flexible docking of peptides to proteins without prior knowledge of the binding site. Nucleic Acids Res 43:W419–W424
16. Blaszczyk M, Kurcinski M, Kouza M, Wieteska L, Debinski A, Kolinski A, Kmiecik S (2016) Modeling of protein–peptide interactions using the CABS-dock web server for binding site search and flexible docking. Methods 93:72–83
17. Jamroz M, Kolinski A, Kmiecik S (2014) Protocols for efficient simulations of long-time protein dynamics using coarse-grained CABS model. Methods Mol Biol 1137:235–250
18. Kar P, Feig M (2014) Recent advances in transferable coarse-grained modeling of proteins. Adv Protein Chem Struct Biol 96:143–180
19. Kolinski A, Bujnicki JM (2005) Generalized protein structure prediction based on combination of fold-recognition with de novo folding and evaluation of models. Proteins 61(Suppl 7):84–90
20. Skolnick J, Zhang Y, Arakaki AK, Kolinski A, Boniecki M, Szilagyi A, Kihara D (2003) TOUCHSTONE: a unified approach to protein structure prediction. Proteins 53(Suppl 6):469–479
21. Debe DA, Danzer JF, Goddard WA, Poleksic A (2006) STRUCTFAST: protein sequence remote homology detection and alignment using novel dynamic programming and profile-profile scoring. Proteins 64:960–967
22. Boniecki M, Rotkiewicz P, Skolnick J, Kolinski A (2003) Protein fragment reconstruction using various modeling techniques. J Comput Aided Mol Des 17:725–738
23. Jamroz M, Kolinski A (2010) Modeling of loops in proteins: a multi-method approach. BMC Struct Biol 10:5
24. Kmiecik S, Jamroz M, Kolinski M (2014) Structure prediction of the second extracellular loop in G-protein-coupled receptors. Biophys J 106:2408–2416
25. Sali A, Blundell TL (1993) Comparative protein modelling by satisfaction of spatial restraints. J Mol Biol 234:779–815
26. Latek D, Kolinski A (2011) CABS-NMR—de novo tool for rapid global fold determination from chemical shifts, residual dipolar couplings and sparse methyl-methyl NOEs. J Comput Chem 32:536–544
27. Kurcinski M, Kolinski A, Kmiecik S (2014) Mechanism of folding and binding of an intrinsically disordered protein as revealed by ab initio simulations. J Chem Theor Comput 10:2224–2231
28. Steczkiewicz K, Zimmermann MT, Kurcinski M, Lewis BA, Dobbs D, Kloczkowski A, Jernigan RL, Kolinski A, Ginalski K (2011) Human telomerase model shows the role of the TEN domain in advancing the double helix for the next polymerization step. Proc Natl Acad Sci U S A 108:9443–9448
29. Kurcinski M, Kolinski A (2007) Hierarchical modeling of protein interactions. J Mol Model 13:691–698
30. Kmiecik S, Gront D, Kouza M, Kolinski A (2012) From coarse-grained to atomic-level characterization of protein dynamics: transition state for the folding of B domain of protein A. J Phys Chem B 116:7026–7032
31. Kmiecik S, Kolinski A (2011) Simulation of chaperonin effect on protein folding: a shift from nucleation-condensation to framework mechanism. J Am Chem Soc 133:10283–10289
32. Kmiecik S, Kolinski A (2008) Folding pathway of the b1 domain of protein G explored by multiscale modeling. Biophys J 94:726–736
33. Kmiecik S, Kurcinski M, Rutkowska A, Gront D, Kolinski A (2006) Denatured proteins and early folding intermediates simulated in a reduced conformational space. Acta Biochim Pol 53:131–144
34. Wabik J, Kmiecik S, Gront D, Kouza M, Kolinski A (2013) Combining coarse-grained protein models with replica-exchange all-atom molecular dynamics. Int J Mol Sci 14:9893–9905
35. Jamroz M, Orozco M, Kolinski A, Kmiecik S (2013) Consistent view of protein fluctuations from all-atom molecular dynamics and coarse-grained dynamics with knowledge-based force-field. J Chem Theor Comput 9:119–125
36. Jamroz M, Kolinski A, Kmiecik S (2013) CABS-flex: server for fast simulation of protein structure fluctuations. Nucleic Acids Res 41:W427–W431
37. Jamroz M, Kolinski A, Kmiecik S (2014) CABS-flex predictions of protein flexibility compared with NMR ensembles. Bioinformatics 30:2150–2154
38. Zambrano R, Jamroz M, Szczasiuk A, Pujols J, Kmiecik S, Ventura S (2015) AGGRESCAN3D

(A3D): server for prediction of aggregation properties of protein structures. Nucleic Acids Res 43:W306–W313

39. McGuffin LJ, Bryson K, Jones DT (2000) The PSIPRED protein structure prediction server. Bioinformatics 16:404–405
40. Xu D, Zhang Y (2011) Improving the physical realism and structural accuracy of protein models by a two-step atomic-level energy minimization. Biophys J 101:2525–2534
41. Eswar N, Webb B, Marti-Renom MA, Madhusudhan MS, Eramian D, Shen M-Y, Pieper U, Sali A (2007) Comparative protein structure modeling using MODELLER. Curr Protoc Protein Sci 2:1–31
42. Claessens M, Van Cutsem E, Lasters I, Wodak S (1989) Modelling the polypeptide backbone with "spare parts" from known protein structures. Protein Eng 2:335–345
43. Gront D, Kmiecik S, Kolinski A (2007) Backbone building from quadrilaterals: a fast and accurate algorithm for protein backbone reconstruction from alpha carbon coordinates. J Comput Chem 28:1593–1597
44. Wang Q, Canutescu AA, Dunbrack RL Jr (2008) SCWRL and MolIDE: computer programs for side-chain conformation prediction and homology modeling. Nat Protoc 3:1832–1847
45. Kmiecik S, Gront D, Kolinski A (2007) Towards the high-resolution protein structure prediction. Fast refinement of reduced models with all-atom force field. BMC Struct Biol 7:43
46. Gront D, Kmiecik S, Blaszczyk M, Ekonomiuk D, Kolinski A (2012) Optimization of protein models. Wiley Interdiscipl Rev-Comput Mol Sci 2:479–493
47. Kim H, Kihara D (2015) Protein structure prediction using residue- and fragment-environment potentials in CASP11. Proteins. doi:10.1002/prot.24920
48. Zimmermann MT, Leelananda SP, Kloczkowski A, Jernigan RL (2012) Combining statistical potentials with dynamics-based entropies improves selection from protein decoys and docking poses. J Phys Chem B 116:6725–6731
49. Faraggi E, Kloczkowski A (2014) A global machine learning based scoring function for protein structure prediction. Proteins 82:752–759
50. Jamroz M, Kolinski A (2013) ClusCo: clustering and comparison of protein models. BMC Bioinformatics 14:62
51. Gront D, Kolinski A (2005) HCPM—program for hierarchical clustering of protein models. Bioinformatics 21:3179–3180
52. Theobald DL, Steindel PA (2012) Optimal simultaneous superpositioning of multiple structures with missing data. Bioinformatics 28:1972–1979
53. Kolinski A, Betancourt MR, Kihara D, Rotkiewicz P, Skolnick J (2001) Generalized comparative modeling (GENECOMP): a combination of sequence comparison, threading, and lattice modeling for protein structure prediction and refinement. Proteins 44:133–149
54. Schwede T, Diemand A, Guex N, Peitsch MC (2000) Protein structure computing in the genomic era. Res Microbiol 151:107–112
55. Raveh B, London N, Schueler-Furman O (2010) Sub-angstrom modeling of complexes between flexible peptides and globular proteins. Proteins 78:2029–2040